



Research article

Quantum chemical determination of molecular geometries and spectral investigation of 4-ethoxy-2, 3-difluoro benzamide

V. Vidhya ^a, A. Austine ^b, M. Arivazhagan ^{c,*}^a Department of Physics, Trichy Engineering College, Trichy, 621132, India^b PG&Research Department of Physics, A.A.Government Arts College, Musiri, 621211, India^c PG&Research Department of Physics, Government Arts College, Trichy, 620022, India

ARTICLE INFO

ABSTRACT

Keywords:

Organic chemistry
Pharmaceutical chemistry
Theoretical chemistry
DFT
NLO
MEP
HOMA index
Dimer

The present work reports the application of density functional theory (DFT) at B3LYP with various basis sets which provide the relationship between the structural and spectral properties of 4-ethoxy-2, 3-difluoro benzamide (4EDFB). A Complete vibrational analysis has been performed at the density functional theory (DFT) method with various basis sets in the ground state. The results of vibrational wave numbers are in good agreement with the experimental spectra (Infrared and Raman). Energy gap of the molecule is evaluated using frontier molecular orbital energies (HOMO-LUMO). The frontier energy gap value reveals the chemical reactivity and intermolecular charge transfer occur within the molecule. Global chemical descriptors provide the local and global softness and local reactivity parameters used to identify the nucleophilic and electrophilic behavior of a specific site within the compound. The dimer structure is performed to evaluate the intermolecular hydrogen bond (O–H–O). The title molecule is capable of receiving second harmonic generation (SHG) is due to high value of hyperpolarizability indicates the NLO activity of the molecule. Apart from NLO entities, aromaticity and the molecular electrostatic potential surface (MEP) explain the hydrogen bonding and provide the reactive behavior of the molecule. The Mulliken population analysis leads to redistribution of electron density in the ring.

1. Introduction

Benzamide derivatives [1, 2] have great pharmaceutical utility, particularly in the treatment of diabetes and show significant antibacterial, antihelmintic, anti-inflammatory, antimarial, antitumor and antiallergic activities as well as used in the preparation of an aromatic ligand. Recently, for Tri-fluoro methyl containing 4-(2-Pyrimidinylamino) benzamides derivatives were evaluated the more potent Hedgehog (Hh) signaling inhibitory activity and Hh signaling pathway which have potential for treatment of many human tumors, such as medulloblastoma ovarian, prostate leukemia lung, pancreatic melanoma, glioblastoma and basal cell carcinoma (BCC). It has been proved that, a range of synthesized di- and triarylbenzamide compounds were tested for their antiproliferative activity as well as their DNA binding activity and 4-Benzoylaminoo-N-(prop-2-yn-1-yl) benzamides are act as novel microRNA-21 (miRNAs) inhibitors for breast cancer. For instance, miR-21 inhibition was alone to suppress tumor cell proliferation in-vitro and could enhance the several types of cancer cells to taxol and much help in chemotherapy and hence it is considered as therapeutic target in

human cancer treatment [3]. The novel heteroaryl-containing benzamide derivatives can be used as a glucokinase activator (GKA) for the treatment of type 2 diabetic mellitus [4, 5, 6]. SOLIAN (4-amino-N-[(1-ethyl pyrrolidin-2-yl) methyl]-5-ethyl sulphonyl-2-methoxy benzamide) is a benzamide derivative chemically related to sulpiride which shows antischizophrenic and antidysthymic drug for the treatment of dysthymic disorders as well as for the determination of amisulphide by HPLC in human plasma analysis with UV absorbance detection [7, 8]. The various halogenated benzamide derivatives used as radiotracers, which played in diagnosing malfunction in dopaminergic neurotransmission [9] have been implicated in a variety of neuropsychiatric disease such as parkinson's disease and drug abuse. Yifan Jin et.al investigated the reaction mechanisms of alkaline hydrolysis of N-(2-methoxyphenyl) benzamide which is used in the chemical industry [10]. Anil Kumar et.al [11] studied the antimicrobial and QSAR studies of substituted benzamides.

Thus, owing to the extensive medical significance of benzamide, this present work decided to interpret the vibrational analysis of 4-ethoxy-2, 3-difluoro benzamide (4EDFB) compound. Recently the vibrational and

* Corresponding author.

E-mail address: jjmarivu@yahoo.co.in (M. Arivazhagan).

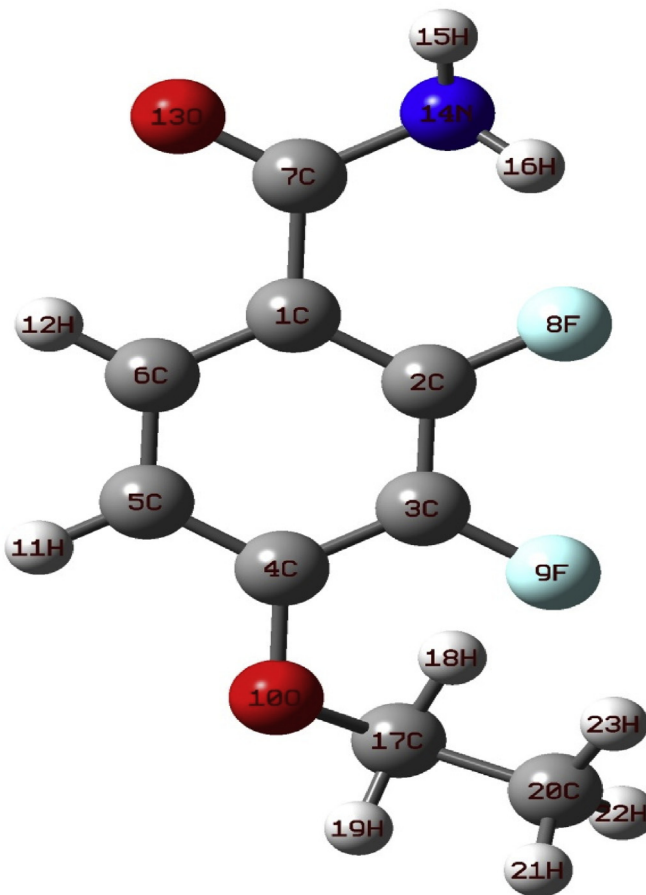


Fig. 1. Optimized Molecular Structure of 4-ethoxy -2, 3-difluoro benzamide.

spectral investigations of 2-fluoro benzamide and 2,6- dichloro benzamide were discussed by using DFT studies [12, 13]. Therefore, In the present investigation, results on the structural and quantum chemical computations of title compound 4-ethoxy-2,3- difluoro benzamide (4EDFB) is reported. In recent years, the interpretations of vibrational and structural characteristics using density functional theory computations have been widely increasing in the pharmaceutical field. Because of this considerations, DFT computations along with vibrational spectroscopic investigations will be employed to determine the complete vibrational assignment on 4-ethoxy-2, 3-difluoro benzamide(4EDFB). Additionally, optimized geometrical parameters, HOMA index, Molecular electrostatic potential, Mulliken charges, Fukui functions, NLO, HOMO-LUMO energy gap and the different electronic properties from the frontier orbitals and hydrogen bond of the little molecule have been performed by using DFT/B3LYP with 6-31+G (d,p)and 6-311++G (d,p) basis sets.

2. Methods

2.1. Experimental

The 4-ethoxy-2, 3-difluoro benzamide (4EDFB) with greater purity was purchased from chemical company and directly used for the spectral measurements without further purification. The FT-IR spectrum was recorded by Nd-YAG laser between 4000 and 400 cm⁻¹ and the FT-Raman spectrum was collected using IFS- 66V model interferometer as excitation wavelength in the range of 3500–50 cm⁻¹.

2.2. Quantum chemical methods

To determine the minimum energy corresponding to most

Table 1
Optimized geometrical parameters of 4 - Ethoxy-2,3-difluoro benzamide.

Parameters	B3LYP Method		
	6-31+G (d,p)	6-311++G (d,p)	XRD*
Bond Length (Å)			
C1–C2	1.395	1.392	1.397
C1–C6	1.407	1.400	1.511
C1–C7	1.507	1.508	1.397
C2–C3	1.393	1.390	
C2–F8	1.361	1.357	1.397
C3–C4	1.402	1.399	
C3–F9	1.357	1.353	1.397
C4–C5	1.407	1.403	1.225
C4–O10	1.350	1.353	1.397
C5–C6	1.386	1.382	
C5–H11	1.085	1.083	
C6–H12	1.084	1.082	1.225
C7–O13	1.230	1.222	1.34
C7–N14	1.363	1.362	
O10–C17	1.450	1.451	1.017
N14–H15	1.009	1.008	1.022
N14–H16	1.007	1.006	
C17–H18	1.092	1.090	
C17–H19	1.092	1.090	
C17–C20	1.522	1.520	
C20–C21	1.094	1.090	
C20–C22	1.096	1.094	
C20–C23	1.094	1.092	
Bond Angle (°)			
C2–C1–C6	116.0	116.1	
C2–C1–C7	126.7	126.8	
C6–C1–C7	117.2	117.1	
C1–C2–C3	122.7	122.6	
C1–C2–F8	121.5	121.6	
C3–C2–F8	115.8	115.8	
C2–C3–C4	120.8	120.8	
C2–C3–F9	117.6	117.7	
C4–C3–F9	121.6	121.5	
C3–C4–C5	117.1	117.1	
C3–C4–O10	126.2	125.9	
C5–C4–O10	116.6	116.9	
C4–C5–C6	121.3	121.3	
C4–C5–H11	117.5	117.5	
C6–C5–H11	121.2	121.2	
C1–C6–C5	122.1	122.1	
C1–C6–H12	117.0	117.0	
C5–C6–H12	120.9	120.9	
C1–C7–O13	120.3	120.3	
C1–C7–N14	118.1	118.0	
O13–C7–N14	121.6	121.7	
C4–C10–C17	122.6	122.3	
C7–N14–H15	117.0	117.0	
C7–N14–H16	123.1	123.2	
H15–N14–H16	119.9	119.8	
O10–C17–H18	110.0	109.99	
O10–C17–H19	102.7	102.7	
O10–C17–C20	112.7	112.7	
H18–C17–H19	108.5	108.5	
H18–C17–C20	111.8	111.7	
H19–C17–C20	110.8	110.8	
C17–C20–H21	110.9	110.9	
C17–C20–H22	109.2	109.2	
C17–C20–H23	111.9	111.9	
H21–C20–H22	108.3	108.3	
H21–C20–H23	108.8	108.7	
H22–C20–H23	107.7	107.6	
Dihedral Angle (°)			
C6–C1–C2–C3	0.17	0.11	
C6–C1–C2–F8	179.5	179.4	
C7–C1–C2–C3	-179.9	-180.0	
C7–C1–C2–F8	-0.53	-0.74	
C2–C1–C6–C5	0.52	0.59	
C2–C1–C6–H12	180.0	-180.0	
C7–C1–C6–C5	-179.5	-179.3	
C7–C1–C6–H12	-0.04	0.09	
C2–C1–C7–O13	-179.4	-179.7	
C2–C1–C7–N14	0.589	-0.12	

(continued on next page)

Table 1 (continued)

Parameters	B3LYP Method		
	6-31+G (d,p)	6-311++G (d,p)	XRD*
C6-C1-C7-O13	0.617	0.16	
C6-C1-C7-N14	-179.4	-180	
C1-C2-C3-C4	-1.04	-1.07	
C1-C2-C3-F9	178.5	178.3	
F8-C2-C3-C4	179.6	179.6	
F8-C2-C3-F9	-0.78	-1.01	
C2-C3-C4-C5	1.16	1.27	
C2-C3-C4-O10	178.0	180.0	
F9-C3-C4-C5	-178.4	-178.1	
F9-C3-C4-O10	-1.53	-1.35	
C3-C4-C5-C6	-0.49	-0.58	
C3-C4-C5-H11	179.6	179.5	
O10-C4-C5-C6	-177.7	-177.6	
O10-C4-C5-H11	2.41	2.51	
C3-C4-O10-C17	28.7	31.9	
C5-C4-O10-C17	-154.4	-151.4	
C4-C5-C6-C1	-0.36	-0.36	
C4-C5-C6-H12	-179.8	-179.7	
H11-C5-C6-C1	179.6	179.5	
H11-C5-C6-H12	0.14	0.15	
C1-C7-N14-H15	179.6	179.3	
C1-C7-N14-H16	0.60	1.33	
O13-C7-N14-H15	-0.43	-0.9	
O13-C7-N14-H16	-179.4	-178.8	
C4-O10-C17-H18	-61.7	-62.8	
C4-O10-C17-H19	-177.1	-178.2	
C4-O10-C17-C20	63.7	62.5	
O10-C17-C20-H21	59.4	55.7	
O10-C17-C20-H22	174.7	175.07	
O10-C17-C20-H23	-66.2	-65.9	
H18-C17-C20-H21	179.9	-179.9	
H18-C17-C20-H22	-60.8	-60.5	
H18-C17-C20-H23	58.3	58.6	
H19-C17-C20-H21	-58.9	-58.7	
H19-C17-C20-H22	60.4	60.6	
H19-C17-C20-H23	179.5	179.7	

For numbering of atoms, refer Fig. 1.

* Experimental data from (12).

conformation of 4EDFB, the potential energy surface (PES) scan along with selected dihedral angle C4– O10–C17–H18 was performed using B3LYP exchange correlation function with 6-31+G (d,p) basis set. Subsequently, structural parameters corresponding to the optimized

geometry and harmonic frequencies for PES minima were found to obtain zero point vibration energy (ZPE) using Gaussian 09W Program at B3LYP with 6-31+G (d,p) and 6-311++G (d,p) basis sets [14]. In recent years B3LYP approach used extensively which gives reliable results of molecules with very satisfactory geometries. The scaled frequencies obtained by the theoretical calculations on the basis of the potential energy distribution (PED) has been done with the MOLVIB program (version 7.0-G77) written by sundius [15] and these normal modes were compared with the experimental FT-IR and Raman spectra of the title compound. In order to predict the stability of the molecule, HOMO-LUMO analysis were examined and the global hardness(η), Chemical potential (μ), electro negativity (χ) have been computed using the highest occupied molecular orbital (HOMO) and lowest unoccupied molecular orbital (LUMO). In order to find the Non Linear optical activity of the molecule (NLO), the dipole moment, polarizability, first and second order hyperpolarizabilities were obtained for future studies. To determine the reactive behavior of the molecule the fukui functions were also reported. Molecular electrostatic potential surface analysis used for predication reactive sites and the positive and negative regions of MEP are related to nucleophilic and electrophilic reactivity. Furthermore, aromaticity of molecule, intermolecular interaction and using Mulliken population analysis, the net charges of the title molecule can be evaluated.

3. Results and discussions

3.1. Potential energy scan

In accordance with the atom numbering scheme of title molecule is given in Fig. 1. The theoretically computed structural parameters are listed in Table 1. In order to obtain the most stable energy of 4EDFB, the detailed potential energy scan profile is performed [16] by choosing the angle C4–O10–C17–H18 that varies in every 60 steps for the angle 180° to get the stable geometry of the molecule and the results are depicted in Fig. 2. The most minimum energy of the present compound is predicted to be -0.243767 a. u at B3LYP/6-31+G (d, p).

3.2. Molecular geometry

The molecule consisting different functions substitutes to the benzene ring causes some changes in structural and electronic properties. From

Scan of Total Energy

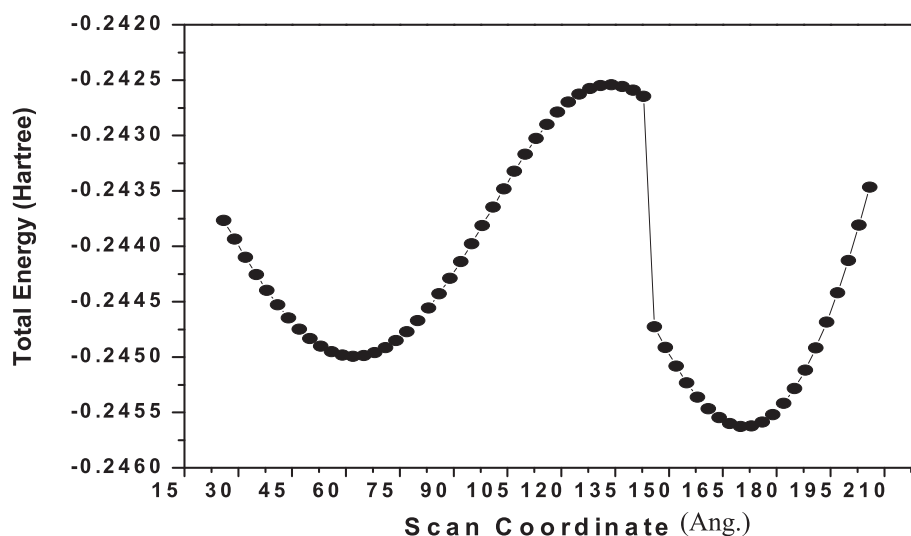


Fig. 2. Scanning profile of 4-ethoxy-2,3-difluoro benzamide.

Table 2

Vibrational assignments of 4 - Ethoxy-2,3-difluoro benzamide along with Observed FT-IR and FT-Raman and calculated (unscaled and scaled) frequencies (cm^{-1}) using B3LYP method with 6-31+G (d,p) and 6-311++G (d,p) basis sets.

S.No	C1 Symmetry	Observed frequencies cm^{-1}		Calculated frequencies cm^{-1}				Assignment with TED %	
				B3LYP/6-31+G (d,p)		B3LYP/6-311++G (d,p)			
		FT-IR	FT Raman	Unscaled	Scaled	Unscaled	Scaled		
1	A	3409	-	3748	3414	3731	3413	ν NH2 ass (98)	
2	A	3200	-	3606	3205	3598	3204	ν NH2 ss (91)	
3	A	-	3125	3230	3131	3211	3131	ν CH ass (97)	
4	A	-	3075	3216	3079	3197	3078	ν CH ss (95)	
5	A	3040	-	3148	3045	3131	3044	ν CH3 ass (99)	
6	A	-	2983	3124	2987	3102	2988	ν CH3ss (97)	
7	A	2961	-	3120	2966	3102	2965	ν CH3ips (95)	
8	A	-	2933	3092	2937	3079	2938	ν CH2ass (97)	
9	A	-	2883	3049	2888	3035	2887	ν CH2ss (96)	
10	A	1734	-	1743	1739	1736	1738	ν C = O (70), bNH(18), CN(10)	
11	A	1654	-	1666	1659	1658	1659	ν CC(60), bCH(20), bNH(15)	
12	A	1641	-	1623	1648	1621	1649	NH2scis (70), ν CC(12)	
13	A	-	1629	1604	1634	1598	1633	ν CC(85), bNH(20)	
14	A	-	1603	1537	1607	1530	1608	ν CC(58), bNH(20)	
15	A	-	1588	1516	1595	1513	1597	CH2sciss (85), bCH(10)	
16	A	1573	-	1503	1581	1497	1583	bCH3(78), bCH2(15)	
17	A	1520	1526	1491	1529	1487	1531	bCH3(92)	
18	A	1467	1462	1484	1466	1477	1467	ν CC(70), bCH(20)	
19	A	-	1436	1425	1440	1420	1439	ν CC(82), bCH2(12)	
20	A	-	1423	1406	1431	1404	1433	CH2 rock (80), bCH2(12)	
21	A	1414	-	1376	1419	1365	1421	ν CN(68), bCH3(22)	
22	A	-	1398	1366	1403	1353	1402	ν CC(75), bCH2(20)	
23	A	1361	-	1320	1367	1321	1369	CH2 wagg (89)	
24	A	1334	-	1302	1338	1292	1336	ν CC(50), bCO(20), bCH(15)	
25	A	-	1308	1233	1315	1229	1315	bCH(90)	
26	A	1294	-	1223	1298	1217	1299	ν CC(72), bCH(30)	
27	A	-	1282	1191	1290	1188	1291	bCH3(85), bCC(10)	
28	A	1227	-	1166	1234	1165	1232	bCH(92)	
29	A	-	1218	1109	1225	1107	1224	bCH3(82)	
30	A	1173	1167	1100	1774	1099	1175	NH2 rock (85)	
31	A	-	1129	1071	1133	1064	1132	ν CO(55), bCH(25)	
32	A	-	1116	1017	1119	1013	1117	ν CO(45), ν CC(25)	
33	A	1107	-	989	1116	991	1115	ω CH(85)	
34	A	1084	-	921	1088	918	1088	ν CF(48), bCC(20)	
35	A	-	1065	883	1068	882	1066	ν CF(35), bCC(20)	
36	A	1027	-	852	1030	854	1031	ω CH(90)	
37	A	934	936	815	940	817	941	ω CH3(85)	
38	A	867	872	768	874	774	876	bC = O (60), bCH(15), bCC(10)	
39	A	800	-	729	808	731	810	bCC(58), ring (20), NH2(10)	
40	A	747	744	694	753	708	755	bCC(40), ring	
41	A	720	718	682	727	682	725	bCN(50), bNH2(20)	
42	A	654	-	627	661	628	660	Rasymd (80), bNH(10)	
43	A	-	642	619	649	620	647	ν bCO(45), bCC(20), bNH(10)	
44	A	627	-	578	635	577	635	NH2wagg (86)	
45	A	-	603	550	611	551	610	Rsymd (85)	
46	A	587	590	531	597	532	597	Rtrigd (78)	
47	A	-	539	503	546	503	546	bCO(48), bCC(30), bCN(10)	
48	A	-	514	458	523	459	524	CH2twist (80)	
49	A	507	-	401	516	402	517	ω CC(45), bCN(12), bC = O (15)	
50	A	-	429	367	435	367	434	bCF(45), bCH3(18)	
51	A	-	386	329	385	330	396	ω CF(48), bCC(30)	
52	A	-	372	314	382	315	383	ω C=O (55), bNH2(15)	
53	A	-	344	297	353	297	350	ω C-O (52), bCH3(15), bCH2(10)	
54	A	-	315	292	324	283	325	NH2 twist (80)	
55	A	-	230	274	239	270	239	t Rsymd65), ω CH(18)	
56	A	-	188	266	197	262	198	ω CF (40, bCC(17))	
57	A	-	-	215	-	213	-	ω CH3(78)	
58	A	-	-	178	-	178	-	ω CO(38), ω CH2(20)	
59	A	-	102	146	111	144	112	ω CF (42), bCH3(30)	
60	A	-	88	104	97	103	98	tRasymd (35), bCC(25)	
61	A	-	60	71	70	65	71	ω CC(50), ring (10)	
62	A	44	-	51	55	44	54	ω CN(60), ω C = O (25)	
63	A	22	-	19	34	21	35	tRtrigd (58)	

Abbreviations: R – ring; ν – stretching; b-in- plane bending; ω – out-of-plane bending; t – torsion; ss-symmetric stretching; ass-asymmetric stretching; ips-in-plane stretching; symd – symmetric deformation; asymd – antisymmetric deformation; trigd – trigonal deformation; sciss: scissoring; rock: rocking; wag:wagging & twist: twisting.

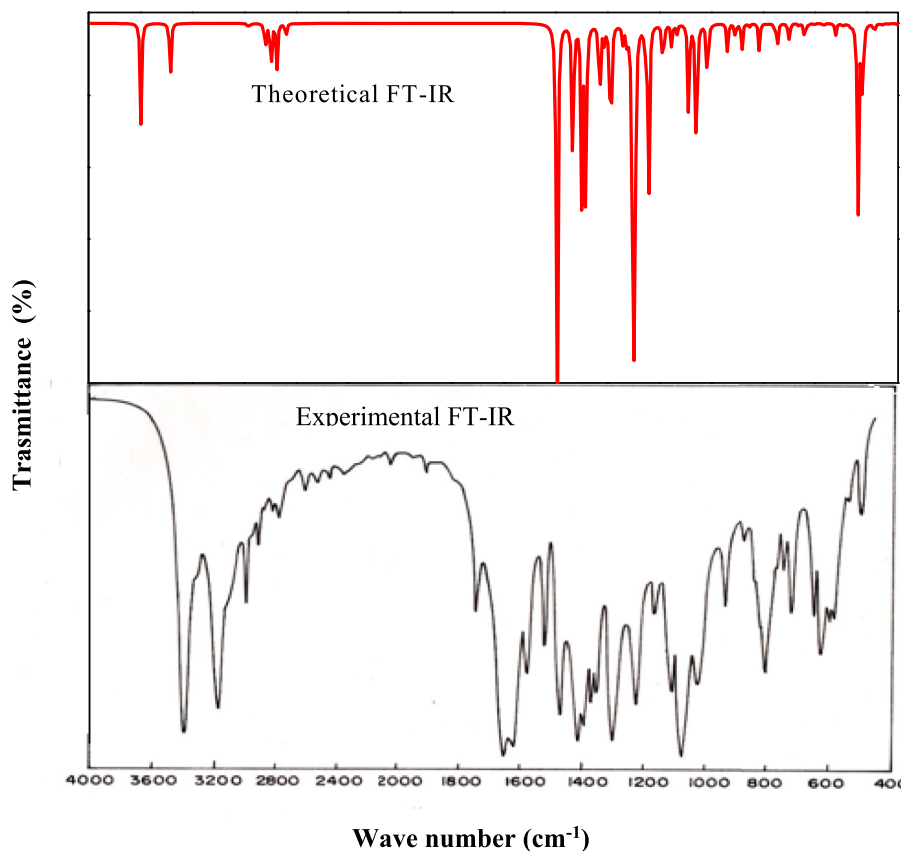


Fig. 3. A combined experimental and theoretical FT-IR spectra of 4-ethoxy - 2, 3-difluoro benzamide.

the computed values, the C-C aromatic distances within the ring are found to be equal around 1.40Å^0 ($\text{C1-C2} = \text{C2-C3} = \text{C5-C6} = \text{C1-C6} = \text{C3-C4} = \text{C4-C5}$) which indicates the indistinctness between the single and double bond due to the π conjugation of electrons [17]. In the case of benzamide, the value of C-C bond length is (1.51Å^0) ($\text{C1-C7} = \text{C17-C20}$) dramatically increases when compared to C-C bond length of the ring is due to no delocalization of electrons. The bond length of functional substituent of benzamide such as methyl ($\text{C-H} = 1.01\text{Å}^0$), methylene ($\text{C-H} = 1.01\text{ Å}^0$) and amide ($\text{N-H} = 1.01\text{Å}^0$) groups are identical which shows the symmetrical arrangement of atoms. The calculated C-N (1.36Å^0) bond length coincides with the actual bond length. Among the C-O bond, the bond length of C1-O10 (1.35Å^0) is shorter due to presenting single and double bond between the carbon and oxygen atoms elucidating the more electrons are participated in the double bond [18]. In the benzene ring, endocyclic C-C-C bond angles are found to be around 120° , among these, a small reduction in two angles ($\text{C2-C1-C6} = 116^\circ.0$ and $\text{C3-C4-C5} = 117^\circ.1$) and small increases in four angles ($\text{C1-C2-C3} = 122^\circ.7$, $\text{C2-C3-C4} = 120^\circ.8$, $\text{C4-C5-C6} = 121^\circ.3$ and $\text{C1-C6-C5} = 122^\circ.1$) are observed due to the substitution in the ring which is not sharing the electrons [12]. However, the variation of the bond angle depends on the factors such as lone pair of electrons in the central atom, size of ligand atoms, electro negativity and hybridization of the central atom. For example, the bond angle decreases when the size of the central atom increases and the bond angle increases when the size of ligand atom increases [19]. The bond angle decreases due to the presence of lone pairs which causes more repulsion on the bond pairs tend to come closer. It is evident that the bond angle C1-C7-O13 ($120^\circ.3$) is little greater than the bond angle C1-C7-N14 ($118^\circ.1$) that shows the oxygen being more electronegative than nitrogen.

From the optimized structural parameters, it is observed that the most of the bond lengths and bond angles are consistent with the earlier

reports [12, 13] and also the optimized bond lengths are coincide well with the bond length obtained by XRD data [12].

3.3. Spectral analysis

The title molecule is non planar which belongs to C1 point symmetry and it consist of 23 atoms that undergoes 63 normal modes of vibrations. The detailed vibrational assignment of fundamental modes computed based on the calculated TED values along with calculated FT-IR and FT-Raman frequencies of title compound which are presented in Table 2. The experimentally recorded and theoretical FT-IR and FT-Raman spectra of 4-ethoxy-2, 3-difluoro benzamide is depicted in Figs. 3 and 4. To obtain better agreement between the calculated and experimental wave numbers the scale factors were applied and discussed below [20, 21]. The comparison of the scaled wave numbers with recorded values demonstrates that the computed at B3LYP method with 6-31+G (d, p)/6-311++G (d,p) basis sets are well consistent with the experimental spectra. The correlation graphic between theoretical and experimental wave numbers are linear which is depicted in Fig. 5 and is defined by the following expressions.

$$\nu_{\text{Cal}} = 0.9978 \nu_{\text{Exp}} + 18.8819 \quad (R^2 = 0.9928) \text{ B3LYP/ 6-31+G(d,p)} \quad (1)$$

$$\nu_{\text{Cal}} = 0.9982 \nu_{\text{Exp}} + 8.71556 \quad (R^2 = 0.9999) \text{ B3LYP/ 6-311++G(d,p)} \quad (2)$$

3.4. Molecular vibrational analysis

3.4.1. NH₂ vibration

Amide group has six normal modes viz., the two stretching vibrations are asymmetric and symmetric stretching modes and four bending

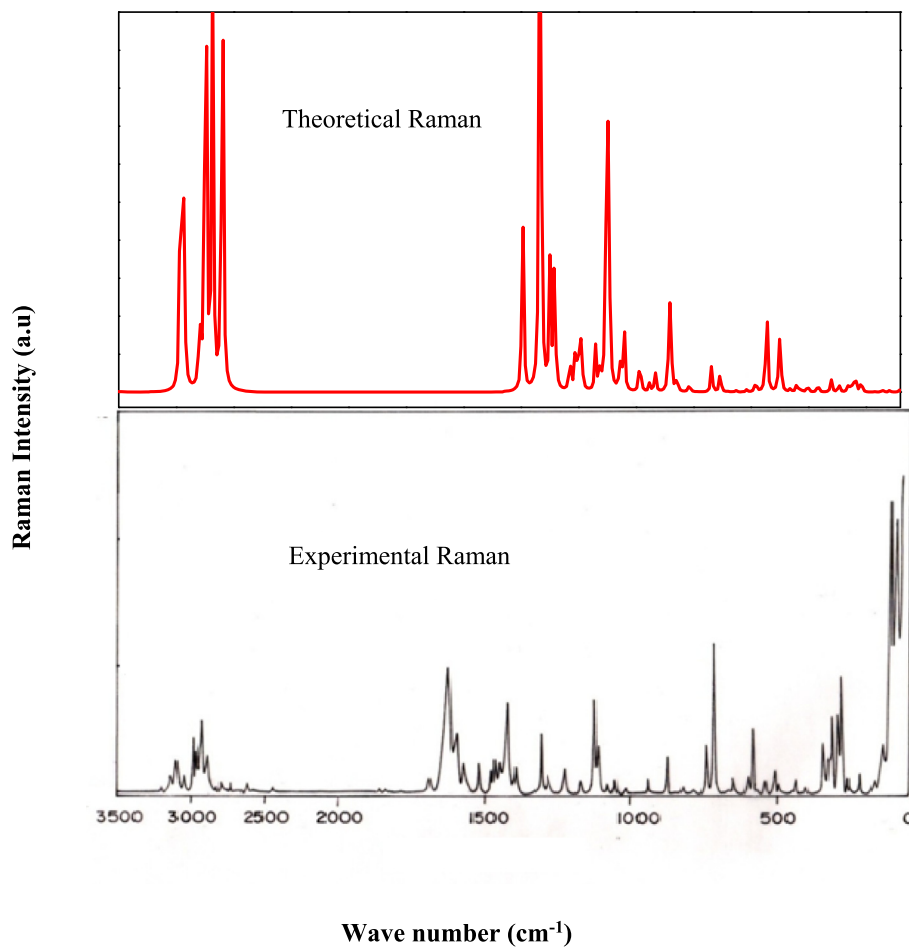


Fig. 4. A combined experimental and theoretical FT-Raman spectra of 4-ethoxy - 2, 3-difluoro benzamide.

vibrations are scissoring, rocking, wagging and twisting modes. Generally asymmetric stretching vibrational mode has higher frequency than symmetric stretching mode. Normally the NH_2 stretching frequency appears in the region $3500\text{-}3300\text{ cm}^{-1}$. For in-plane- bending, the wave numbers are appear at $1700\text{-}1600\text{ cm}^{-1}$ and $1150\text{-}900\text{ cm}^{-1}$ for out-of-plane bending deformations [22]. In 2-ethylpyridine-4-carbothioamide, the stretching modes are occurring at 3430cm^{-1} and 3440 cm^{-1} in IR and Raman spectra, respectively [23]. Wysokinski et. al. have observed these modes at $3352\text{/}3240\text{ cm}^{-1}$ in IR and $3350\text{/}3236\text{ cm}^{-1}$ in Raman spectra for 4-thiocarbamoyl pyridine [24]. Yilmaz et al have assigned the asymmetric and symmetric stretching wave numbers at 3373 cm^{-1} and 3265 cm^{-1} for prothionamide [25]. In the present investigation, the title molecule consist only one NH_2 group. The two NH_2 stretching modes assigned at 3409 cm^{-1} and 3200 cm^{-1} for as asymmetric stretching and symmetric stretching modes in the FT-IR spectrum [12]. The bending vibrations are assigned at 1173 cm^{-1} , 1641 cm^{-1} and 1167 cm^{-1} to NH_2 scissoring and rocking vibrations in the FT-IR and FT- Raman spectra and twisting and wagging modes are observed at 627cm^{-1} (IR) and 315 cm^{-1} (R) respectively.

3.4.2. C-H vibrations

The aromatic compounds show that the C-H stretching wave numbers are not affected by the nature of substituents, they commonly exhibit in the region $3100\text{-}3000\text{ cm}^{-1}$ [12,26]. The C-H stretching mode was observed at 3107 cm^{-1} in FT-IR and at 3070 cm^{-1} in FT-Raman for 3, 5-difluoroaniline by Pathak et.al [34]. In the present investigation, the C-H stretching vibrations are attributed at 3125 cm^{-1} and 3075 cm^{-1} of title compound. The C-H in-plane bending vibrations lie in the region $1000\text{-}1300\text{ cm}^{-1}$ and the C-H out-of -plane bending vibrations are

expected in the frequency range $750\text{-}100\text{ cm}^{-1}$ [27]. For the title compound, in -plane bending wave numbers are observed at 1227cm^{-1} in FT-IR and in Raman spectrum at 1308 cm^{-1} . The bands observed at 1107cm^{-1} and 1027 cm^{-1} in the FT Raman spectra are assigned to C-H out - of-plane bending vibration.

3.4.3. CH_2 vibrations

The vibrations of CH_2 group has six fundamental modes that can be associated to each CH_2 group namely asymmetric stretching and symmetric stretching, scissoring and rocking belongs to in-plane bending vibrations and two out-of -plane bending vibrations are twisting and wagging. The CH_2 stretching vibration generally expected in the region $3000\text{-}2800\text{ cm}^{-1}$. The asymmetric and symmetric stretching bands corresponding to wave numbers of methylene (CH_2) group appear normally in the expected region $3000\text{-}2900\text{ cm}^{-1}$ and $2900\text{-}2800\text{ cm}^{-1}$ [28]. Ramkumar et. al [29]. has reported the CH_2 asymmetric stretching at 2968 cm^{-1} in FT-Raman spectrum. CH_2 scissoring and wagging modes are attributed in the region at 1651 cm^{-1} and 1465 cm^{-1} in FT-IR spectrum. Vesna et.al [30].assigned the bands at 2978 and 2806 cm^{-1} to methylene asymmetric and symmetric stretching vibrations. For 4EDFB, CH_2 asymmetric and symmetric stretching vibrations assigned at 2933 cm^{-1} and 2883 cm^{-1} in FT-Raman spectrum. The bending vibrations of CH_2 scissoring, rocking, wagging and twisting modes are appear in the expected frequency region $1500\text{-}800\text{ cm}^{-1}$ which is revealed to couple with C-C and C-N stretching vibrations. The modes assigned at 1588 cm^{-1} and 1423cm^{-1} for scissoring and rocking modes in FT-Raman spectrum. The wagging and twisting modes are expected at 1361 cm^{-1} and 514 cm^{-1} in FT-IR and FT-Raman spectrum, respectively.

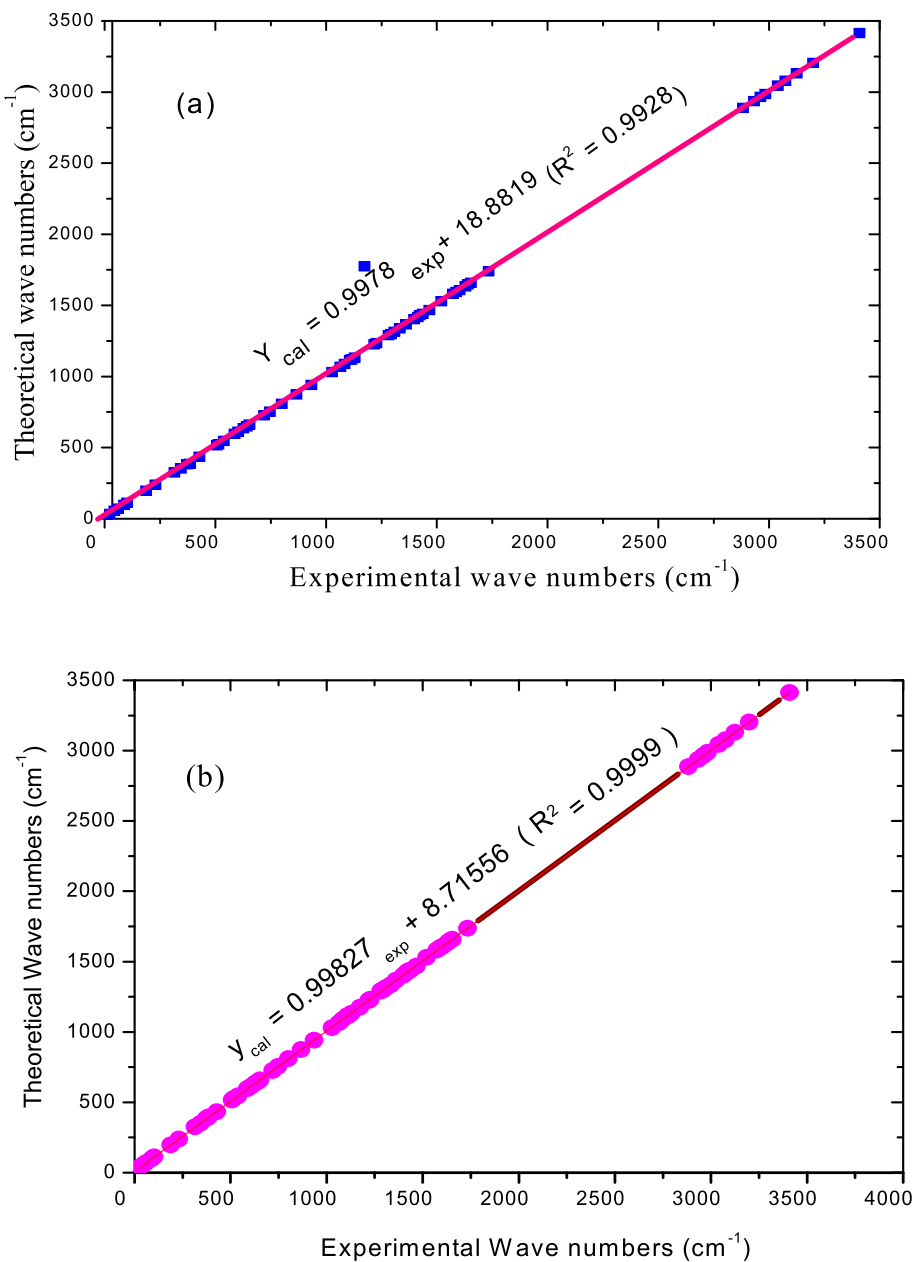


Fig. 5. Comparison of experimental and theoretical wave numbers for different basis sets of 4- ethoxy - 2, 3-difluoro benzamide. (a) B3LYP/6-31+G (d, p) and (b) B3LYP/6-311++G (d, p).

3.4.4. CH₃ vibrations

Methyl group attached along with methylene and oxygen atom to benzene ring. Methyl group vibrations are electron-donating substituent and can vibrate in nine different ways viz., CH₃-symmetric and asymmetric stretching, in-plane and out-of- plane bending modes and CH₃ torsion. Methyl C-H stretching mode appears at lower frequencies than those aromatic ring at 3000-2900 cm⁻¹. The anti-symmetric and symmetric deformations of the methyl group attributed in the region 1465-1440 cm⁻¹ and 1040-990 cm⁻¹ respectively [31, 32]. In the present investigation, the asymmetric stretching mode appear at 3040cm⁻¹ and 2983 cm⁻¹ in the FT-IR and FT-Raman spectrum, respectively, and symmetric stretching mode appear at 2961 cm⁻¹ in the FT- Raman spectrum. The methyl rocking mode vibration usually appears within the region 1070-1010 cm⁻¹. The CH₃ rocking and torsional vibrations are assigned which listed in Table 2.

3.4.5. C-F vibrations

The C-F stretching modes are difficult to determine which is due to coupling with other bending modes of vibration. The C-F stretching modes are obtained for several fluoro benzenes in the region 1000-1300 cm⁻¹ which are strongly coupled with C-H in - plane bending vibrations [33]. In this compound the two fluorine atoms are attached in the position of ortho and meta places of the parent ring. In 3, 5-difluoroaniline, Pathak et.al [34]. observed the C-F stretching modes that are coupled with C-N and C-C stretching vibrations and C-H in-plane bending vibrations are assigned at 1355 cm⁻¹ (IR) and 1348 cm⁻¹ (R) and 1115 cm⁻¹ (IR) and 1113 cm⁻¹ (R). Accordingly for 4EDFB, the C-F stretching vibration observed at 1080 cm⁻¹ and 1065 cm⁻¹ in Raman spectrum. For the present compound, the heavy substituents are attached to fluorine atoms tend to shift the C-F stretching modes to lower wave numbers. These wave numbers are coinciding well with earlier reports [35, 36]. Generally, the C-F in-plane bending vibration is obtained at 250 -350

cm^{-1} . For 4EDFB, the C–F in-plane and out-of-plane vibrations are obtained at 429 cm^{-1} , 386 cm^{-1} and 188 cm^{-1} and 102 cm^{-1} in FT-Raman spectrum respectively.

3.4.6. C–C vibrations

The carbon atom in the benzene ring undergoes coupled vibration due to presence of conjugate substituent which give maximum C–C stretching modes of four bands that appear in the region $1660\text{--}1420 \text{ cm}^{-1}$ [37]. In general, Varsanyi assigned that the variable intensity of five bands can be observed at $1625\text{--}1590 \text{ cm}^{-1}$, $1590\text{--}1575 \text{ cm}^{-1}$, $1540\text{--}1470 \text{ cm}^{-1}$, $1460\text{--}1430 \text{ cm}^{-1}$ and $1380\text{--}1280 \text{ cm}^{-1}$, in this region [38]. For 4EDFB, the bands obtained at 1654 cm^{-1} , 1629 cm^{-1} , 1603 cm^{-1} , 1467 cm^{-1} , 1462 cm^{-1} , 1436 cm^{-1} , 1398 cm^{-1} , 1334 cm^{-1} , and 1294 cm^{-1} in the FT-IR and FT-Raman spectrum are assigned to the C–C stretching modes. The C–C in-plane and out-of-plane bending vibrations are usually obtained in the range at $1000\text{--}675 \text{ cm}^{-1}$ and $450\text{--}112 \text{ cm}^{-1}$. In the present compound, the wave numbers of in-plane and out-of-plane bending vibrations are observed which are listed in Table 2.

3.4.7. C–N vibrations

It is very difficult to identify the C–N vibration due to the possible mixing of several bands. The C–N Stretching vibrations appear in the region $1200\text{--}1400 \text{ cm}^{-1}$. Polat et.al [39] reported the C–N stretching vibrations in the region $1300\text{--}1350 \text{ cm}^{-1}$ for the imidazole ring. For 4EDFB, the C–N stretching vibration has observed at 1414 cm^{-1} in FT-IR spectrum. For 6-dichlorobenzamide, Yaping Tao et.al [13] have obtained the C–N in-plane and out-of-plane bending vibrations at 571 cm^{-1} and 74 cm^{-1} . For 4EDFB, the C–N bending vibrations are observed at 720 cm^{-1} (IR) 718 cm^{-1} (R) and 44 cm^{-1} (IR). The experimental values of C–N stretching and bending modes show good agreement with theoretical values.

3.4.8. C=O and C–O vibrations

The Carbonyl stretching C=O vibrations are appear in the region of $1850\text{--}1600 \text{ cm}^{-1}$ [16]. The IR bands located at 1734 cm^{-1} for C=O stretching vibration and the bands obtained at 1129 cm^{-1} and 1116 cm^{-1} for C–O stretching vibrations in FT-Raman spectrum. The C=O and C–O in-plane and out-of-plane bending vibrations have been identified and are labeled in Table 2. These values are in good agreement with the theoretical calculations performed at B3LYP with various basis sets.

3.5. Scale factors

The quantum chemical calculation reveals the overestimated calculated vibrational modes when compared to the experimental values due to the anharmonicity that can be corrected by introducing scale factors to minimize overall deviation using MOLVIB 7.0 by sundius [20]. The Root Mean Square (RMS) values of IR and Raman wave numbers were evaluated using the following equation [40, 41].

$$\text{RMS} = \sqrt{\frac{1}{n-1} \sum_i^n (v_i^{\text{calc}} - v_i^{\text{exp}})^2} \quad (3)$$

The RMS errors are found to be 106.6 cm^{-1} at B3LYP/6-31+G (d,p) for unscaled frequencies and hence to scale down the calculated vibrational frequency along with the experimental ones, the scale factors are refined that resulted in to the RMS deviation of 6.61 cm^{-1} between the experimental and scaled quantum wave numbers. The selective scale factors for present molecule are predicted to be 0.898 for N–H stretching, 0.956 for C–H stretching and 0.892 for bending vibrations (in-plane and out-of-plane).

3.6. Aromaticity

The analysis of aromatic character is considered as one of the most fundamental concepts in current chemistry by which the special stability

Table 3

The calculated entities of HOMA index of 4-Ethoxy-2,3-difluoro benzamide using B3LYP/6-31+G (d, p).

parameters	R_{ava}	R_{opt}	α	GEO	EN	HOMA
Values (Å^0)	1.398	1.388	257.7	0.0153	0.0258	0.9589

of benzene is explained. Elucidation of aromaticity depends on various significant categories and the main criteria of aromaticity are:

- (i) Structural – bond length equalization.
- (ii) Energetic – increased stability.
- (iii) Negative Nucleus Independent Chemical shift (NICS) – remarkable chemical shift.
- (iv) Magnetic – high magnetic anisotropies.

Harmonic Oscillator Model of Aromaticity (HOMA) is the most significant indicator to express geometrical aspects of aromaticity of π -electron molecules. Decrease of aromaticity of the molecule can be realized by two different categories namely GEO and EN respectively. Here GEO is defined as an increase of the bond distance alteration and EN is the extension of the mean bond distance. These two characteristics have been discovered due to the applications of the HOMA index as described by Krygowski et. al [42, 43, 44].

The HOMA index is expressed as [45]:

$$\text{HOMA} = 1 - [\alpha (R_{\text{opt}} - R_{\text{av}})^2 + \frac{\alpha}{n} \sum (R_{\text{av}} - R_i)^2] \quad (4)$$

$$= 1 - \text{EN} - \text{GEO} \quad (5)$$

where

$$\text{EN} = \alpha (R_{\text{opt}} - R_{\text{av}})^2 \quad (6)$$

$$\text{GEO} = \frac{\alpha}{n} \sum (R_{\text{av}} - R_i)^2 \quad (7)$$

Here, n is the total number of bonds, R_i stands for running bond length, R_{av} stands for the average bond length and α (for C–C bonds $\alpha = 257.7$) is an empirical constant fixed to HOMA = 0 and HOMA = 1 for the system with equal bonds to optimal value R_{opt} (for C–C bonds $R_{\text{opt}} = 1.388 \text{ Å}^0$) considered for fully aromatic systems. The HOMA index can be smaller than 1 for compounds with $R_{\text{ave}} > R_{\text{opt}}$. For instance, the reported value of HOMA index of 3-amino-4-methoxy benzamide is 0.9812 [40]. The calculated entities of the HOMA index for the present molecule have been presented in Table 3. The presented value shows that there was no deviation from aromaticity.

3.7. Frontier molecular orbital analysis

The molecular orbital energies are efficient tools which play crucially in the electric and optical properties as well as in quantum chemistry. The conjugated molecules are described by the two important orbitals named as HOMO and LUMO. They are known as frontier molecular orbitals (FMO) that lie at the outer most boundaries of the electrons of the molecules [46]. The frontier molecular orbital elucidates several types of reactions, particularly one electron excitation from the highest occupied molecular orbital (HOMO) to the lowest unoccupied molecular orbital (LUMO). The HOMO energy measures the electron-donar character while the LUMO energy measures the electron-acceptor character. The greater electron-donor capacity indicates the greater value of HOMO energy and the lower value of LUMO energy indicates the lower resistance to accept electrons. The frontier energy separation between the HOMO and LUMO is an important parameter in determining molecular electrical transport properties and also elucidate the kinetic stability, chemical reactivity and optical polarizability of the molecules. In order to determine the energetic behavior of the title molecule, the HOMO-LUMO energy have been

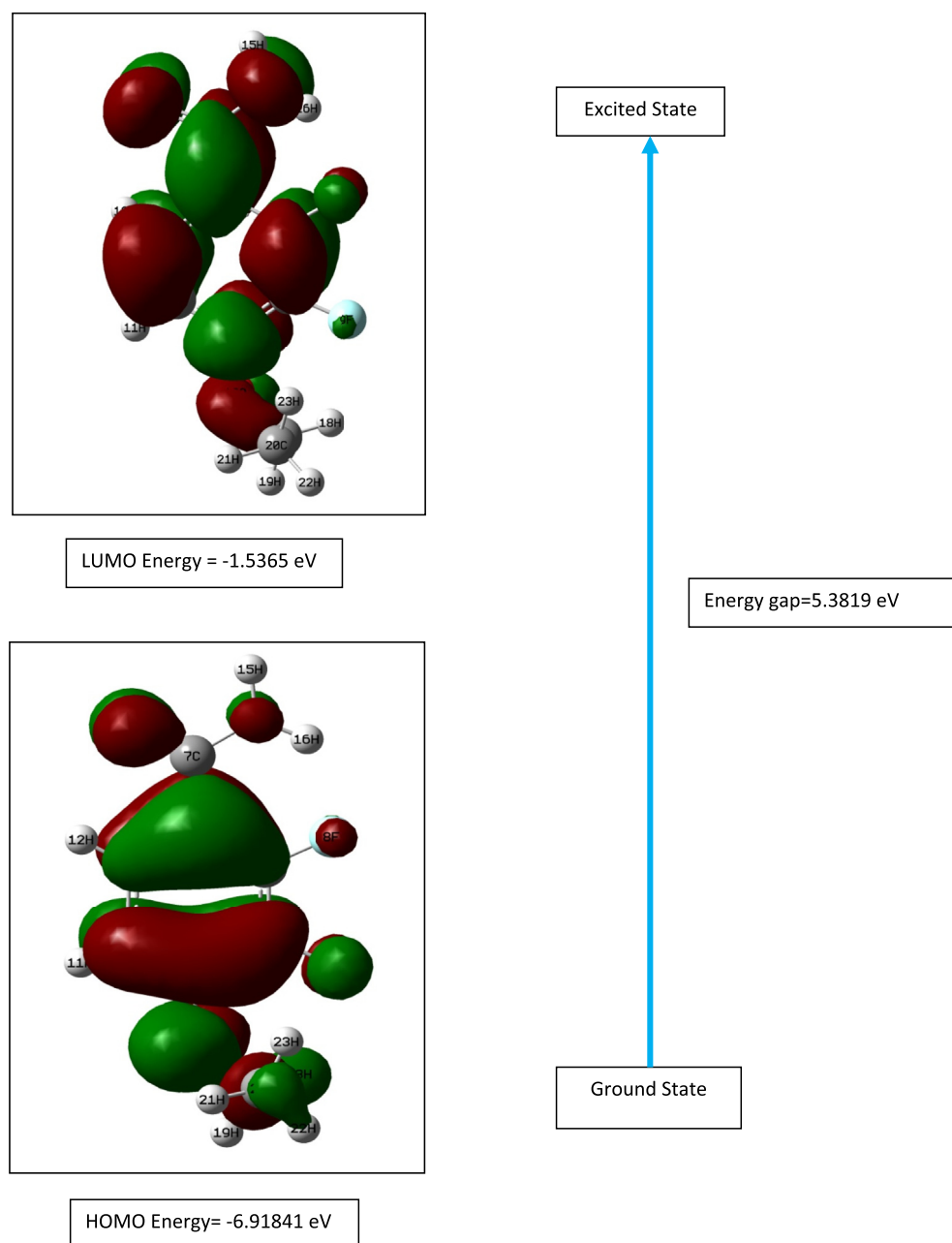


Fig. 6. Pictorial representation of HOMO and LUMO of 4-ethoxy -2, 3-difluoro benzamide.

done using B3LYP/6-31+G (d,p) basis set. The pictorial representation of HOMO-LUMO is labeled in Fig. 6. The HOMO-LUMO plot describes the information about physical properties of molecules and provides insight in to the nature of the reactivity. HOMO is localized over entire molecule except hydrogen atoms and LUMO is delocalized on the entire molecule except ethoxy group of the molecule [47]. The Color codes of red to green indicate the positive and negative phase of the molecule. The frontier molecular orbital energy gap ($E_{\text{LUMO}} - E_{\text{HOMO}}$) is significant to imply the molecular stability with respect to further chemical reaction. In this case, the energy gap of HOMO and LUMO is predicted to be 5.38191eV. The HOMO-LUMO gap of 6-dichlorobenzamide is found to be 5.944 eV [13]. A large value of frontier orbital gap is associated with a low chemical reactivity and eventual charge transfer occurs within the compound [48, 49]. The molecule with large HOMO-LUMO gap means less polarizable and chemically stable compound.

HOMO Energy = -6.91841eV

LUMO Energy = -1.5365 eV

Energy gap $\Delta E = 5.38191$ eV

3.8. Global chemical descriptors

The concept of chemical reactivity of molecule is related to a large part theoretical chemistry which is based on the frontier molecular orbital theory. The density functional theory has extraordinary potential to obtain the global reactivity descriptor which implies the information about the general behavior of the molecules [50]. These are the electronic chemical potential (μ), hardness (η), and softness (s), electronegativity (χ) and elecrophilicity (ω). Global hardness measures the resistance of an atom to a charge transfer and softness describes the

Table 4Calculated parameters of S and ω of 4 - Ethoxy-2,3-difluoro benzamide using B3LYP/6-31+G (d,p).

METHOD/BASIS SET DFT/ B3LYP	Molecular Properties (eV)	Ionization Potential	Electron Affinity	Electro negativity	Chemical Potential	Hardness	Softness	Electrophilicity
		I	A	χ	μ	η	S	ω
Definition		-E _{HOMO}	-E _{LUMO}	$\chi = [(I + A)/2]$	$\mu = -(I + A)/2$	$\eta = [(I - A)/2]$	$S = 1/2\eta$	$\omega = \mu^2/2\eta$
Values in a.u	0.25175	0.05453	0.15314	-0.15314	0.09861	0.14096	0.118912	
Values in e.V	6.91841	1.5365	4.227455	-4.227455	2.690955	0.371615	3.320638	

ability of an atom to receive electrons.

According to Euler-Lagrange equation in density functional theory, the general,

definitions [51] of chemical parameters are shown to be

$$\mu = \left(\frac{\partial E}{\partial N} \right) = -\frac{1}{2}(I - A) \quad (8)$$

$$\eta = \left(\frac{\partial \mu}{\partial N} \right) v(r) = \left(\frac{\partial^2 \mu}{\partial N^2} \right) v(r) = I - A \quad (9)$$

Where, E, N and η are energy, number of electrons and external potential of the system, respectively.

The global softness, S is simply the reciprocal of the global hardness which measures the extent of chemical reactivity.

$$S = \eta^{-1} = \left(\frac{\partial N}{\partial \mu} \right)_{v(r)} \quad (10)$$

Most part of theoretical chemistry, is related to reactivity which is based on the concepts of frontier molecular orbital energies such as highest occupied molecular orbital (HOMO) and the lowest unoccupied molecular orbital. According to Koopmans's theorem, Ionization potential (I) and the electron affinity (A) are related to the energies of HOMO and LUMO, respectively.

And the above equations can be modified and are defined as

$$\text{Chemical potential } \mu = -\left(\frac{I + A}{2} \right) \quad (11)$$

$$\text{Global hardness } \eta = \left(\frac{I - A}{2} \right) \quad (12)$$

$$\text{Electro negativity } \chi = \left(\frac{I + A}{2} \right) \quad (13)$$

The global electrophilicity index ω can be described using μ & η as follows.

$$\omega = \frac{\mu^2}{2\eta} \quad (14)$$

This new reactivity index measures the stabilization in energy. The evaluated chemical descriptors of EHOMO, ELUMO, μ , λ , η , χ , S and ω for 4EDFB are summarized in Table 4. The calculated results show that, the negative chemical potential value is $\mu = -4.2275$ eV and indicates more stability of the title molecule. Global hardness measures the reactivity and softness and describes the ability of an atom to receive electrons. A good electrophile described by a large value of electrophilicity while good nucleophile described by a small value of nucleophilicity [52, 53].

3.9. Local reactivity descriptors

3.9.1. Fukui function

Apart from the global properties, the two local reactivity parameters such as fukui function and local softness are necessary for difference treating the reactive behavior of atoms in forming molecule. The fukui function or frontier function used to predict the reactivity sites in a molecule and to determine electrophilic and nucleophilic attack, respectively.

Table 5

Calculated fukui functions of 4 - Ethoxy-2,3-difluoro benzamide using B3LYP/6-31+G (d,p) Method.

Atom	Neutral (a.u)	Cation (N+1) (a.u)	Anion (N-1) (a.u)	f ⁺ _k (a.u)	f _k (a.u)	f ⁰ _k (a.u)	Δf _(k) (a.u)
C1	0.9682	0.7248	0.6167	-0.2434	0.3514	0.0540	-0.5948
C2	-0.7525	-0.3820	-0.2959	0.3706	-0.4566	-0.0430	0.8272
C3	0.9181	1.0212	0.2881	0.1031	0.6300	0.3665	-0.5269
C4	-0.2600	-0.2489	-0.6250	0.0111	0.3650	0.1881	-0.3539
C5	0.1000	0.1020	0.5189	0.0019	-0.4188	-0.2085	0.4207
C6	-0.5441	-0.6710	-0.6849	-0.1269	0.1408	0.0070	-0.2677
C7	0.5177	0.5306	0.5150	0.0130	0.0027	0.0078	0.0103
F8	-0.3619	-0.3022	-0.3886	0.0597	0.0266	0.0432	0.0331
F9	-0.3647	-0.3135	-0.3785	0.0512	0.0138	0.0325	0.0374
O10	-0.3580	-0.2134	-0.3505	0.1446	-0.0075	0.0685	0.1521
H11	0.1456	0.1971	0.0947	0.0514	0.0509	0.0512	0.0005
H12	0.1770	0.2100	0.1358	0.0329	0.0412	0.0371	-0.0083
O13	-0.5391	-0.3657	-0.6404	0.1734	0.1013	0.1374	0.0722
N14	-0.5951	-0.4803	-0.5897	0.1148	-0.0054	0.0547	0.1201
H15	0.3325	0.3585	0.2774	0.0260	0.0551	0.0406	-0.0291
H16	0.3175	0.3283	0.2873	0.0108	0.0303	0.0205	-0.0195
C17	-0.0600	-0.0454	0.0667	0.0146	-0.1267	-0.0560	0.1413
H18	0.1603	0.1835	0.1371	0.0233	0.0232	0.0232	0.0001
H19	0.1483	0.1953	0.1067	0.0470	0.0415	0.0443	0.0055
C20	-0.4245	-0.3835	-0.5248	0.0410	0.1003	0.0707	-0.0593
H21	0.1615	0.1872	0.1431	0.0257	0.0184	0.0221	0.0074
H22	0.1543	0.1960	0.1197	0.0417	0.0346	0.0382	0.0070
H23	0.1590	0.1714	0.1712	0.0124	-0.0122	0.0001	0.0245

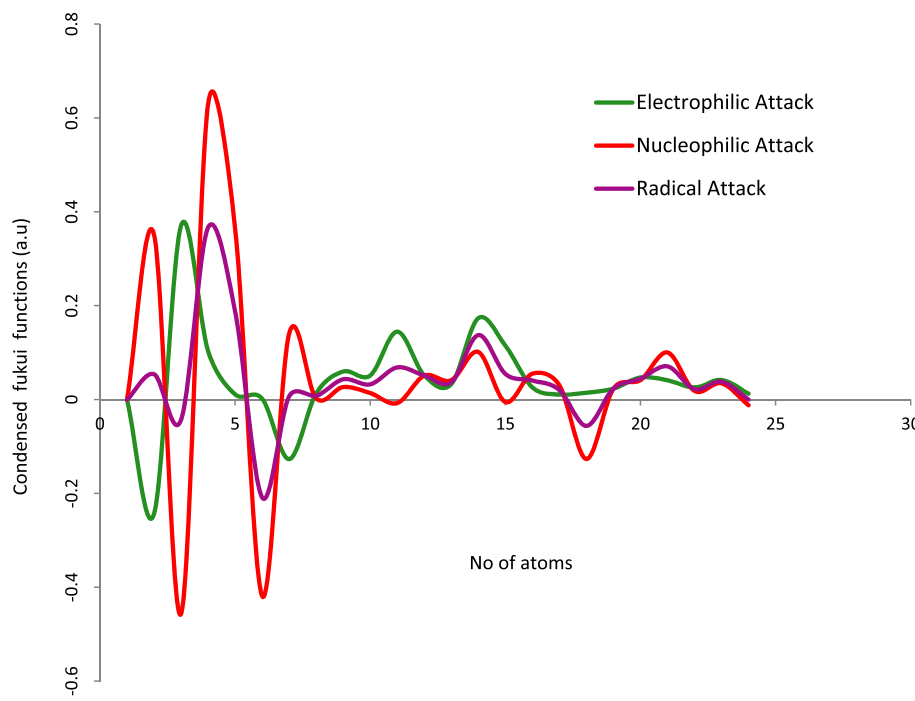


Fig. 7. Variation of condensed fukui functions for different atoms of 4-ethoxy -2, 3-difluoro benzamide.

The condensed form of the fukui function for an atom k in a molecule can be defined as [54, 55].

$$f_k^+ = q_k^{(N+1)} - q_k^{(N)} \text{ for molecule k as an electrophile} \quad (15)$$

$$f_k^- = q_k^{(N)} - q_k^{(N-1)} \text{ for molecule k as an nucleophile} \quad (16)$$

$$f_{k0} = q_k^{(N+1)} - q_k^{(N-1)} \text{ for molecule k as a radical} \quad (17)$$

Where the parameters $q_k^{(N)}$, $q_k^{(N+1)}$ and $q_k^{(N-1)}$ are the charges of molecule k, N, (N-1) and (N+1) electrons for neutral, anion and cation, respectively at the optimized geometry of the molecule with N electrons. In order to determine the pin point distribution of the atomic sites on the molecule, the Fukui function was characterized through above three equations which evaluate the reactivity at atomic resolution. In this case,

mulliken population analysis was used to calculate the fukui function of the title molecule at B3LYP/6-31+G (d, p) basis set. The evaluated reactivity parameters results exhibit that the more reactive sites for electrophile is C3 = 0.6300, nucleophile is C3 = 0.33706 and radical is C2 = 0.827198 a. u [56, 57] which are reported in Table 5 and the graphical representation is shown in Fig. 7.

3.9.2. Local softness

Local softness is extensively successful tool in determining the site selectivity and regio chemistry. A mutually related reactivity parameters of fukui function $f(r)$ and local softness $s(r)$ can be written as

$$s(r) = S f(r) \quad (18)$$

The local softness describes the reaction path and discovers the type

Table 6
Calculated Local reactivity parameters of 4-ethoxy -2, 3-difluoro benzamide using B3LYP/6-31+G (d,p) Method.

Atoms	S^+_{ik} (a.u)	S^-_{ik} (a.u)	S^0_{ik} (a.u)	ΔS_{ik} (a.u)	ω^+_{ik} (a.u)	ω^-_{ik} (a.u)	ω^0_{ik} (a.u)	$\Delta \omega_{ik}$ (a.u)	Electrophilicity (a.u)	Nucluophility (a.u)
C1	-2.4589	3.5504	0.5457	-6.0093	-0.0296	0.0428	0.0066	-0.0725	-0.6926	-1.4439
C2	3.7436	-4.6132	-0.4348	8.3568	0.0451	-0.0556	-0.0052	0.1008	-0.8115	-1.2323
C3	1.0416	6.3645	3.7031	-5.3229	0.0126	0.0767	0.0446	-0.0642	0.1637	6.1105
C4	0.1122	3.6874	1.8998	-3.5752	0.0014	0.0445	0.0229	-0.0431	0.0304	32.8677
C5	0.0194	-4.2312	-2.1059	4.2506	0.0002	-0.0510	-0.0254	0.0512	-0.0046	-218.2527
C6	-1.2818	1.4225	0.0704	-2.7043	-0.0155	0.0172	0.0008	-0.0326	-0.9010	-1.1098
C7	0.1312	0.0273	0.0792	0.1039	0.0016	0.0003	0.0010	0.0013	4.8081	0.2080
F8	0.6033	0.2692	0.4363	0.3342	0.0073	0.0032	0.0053	0.0040	2.2414	0.4462
F9	0.5170	0.1393	0.3282	0.3777	0.0062	0.0017	0.0040	0.0046	3.7105	0.2695
O10	1.4609	-0.0761	0.6924	1.5369	0.0176	-0.0009	0.0083	0.0185	-19.2064	-0.0521
H11	0.5196	0.5145	0.5170	0.0051	0.0063	0.0062	0.0062	0.0001	1.0098	0.9903
H12	0.3326	0.4165	0.3746	-0.0839	0.0040	0.0050	0.0045	-0.0010	0.7986	1.2522
O13	1.7522	1.0233	1.3877	0.7289	0.0211	0.0123	0.0167	0.0088	1.7124	0.5840
N14	1.1597	-0.0541	0.5528	1.2138	0.0140	-0.0007	0.0067	0.0146	-21.4319	-0.0467
H15	0.2629	0.5567	0.4098	-0.2938	0.0032	0.0067	0.0049	-0.0035	0.4722	2.1178
H16	0.1086	0.3057	0.2072	-0.1971	0.0013	0.0037	0.0025	-0.0024	0.3553	2.8145
C17	0.1477	-1.2801	-0.5662	1.4278	0.0018	-0.0154	-0.0068	0.0172	-0.1154	-8.6639
H18	0.2349	0.2341	0.2345	0.0008	0.0028	0.0028	0.0028	0.0000	1.0032	0.9968
H19	0.4751	0.4194	0.4472	0.0557	0.0057	0.0051	0.0054	0.0007	1.1328	0.8827
C20	0.4146	1.0132	0.7139	-0.5986	0.0050	0.0122	0.0086	-0.0072	0.4092	2.4440
H21	0.2601	0.1858	0.2229	0.0743	0.0031	0.0022	0.0027	0.0009	1.3997	0.7145
H22	0.4209	0.3500	0.3855	0.0709	0.0051	0.0042	0.0046	0.0009	1.2026	0.8315
H23	0.1252	-0.1228	0.0012	0.2479	0.0015	-0.0015	0.0000	0.0030	-1.0198	-0.9806

Table 7

The Calculated values of Dipole Moment, Polarizability, Anisotropic Polarizability, First Hyper Polarizability and Second Order Polarizability of 4-Ethoxy 2,3-difluoro benzamide.

Dipole Moment (μ /D)		Polarizability (α)		Anisotropic Polarizability ($\Delta\alpha$)		First Hyper Polarizability (β)		Second Order Polarizability (γ)	
B3LYP/6-31+G (d,p)	B3LYP/6-31+G (d,p)	B3LYP/6-31+G (d,p)	B3LYP/6-31+G (d,p)	B3LYP/6-31+G (d,p)	B3LYP/6-31+G (d,p)	B3LYP/6-31+G (d,p)	B3LYP/6-31+G (d,p)	B3LYP/6-31+G (d,p)	B3LYP/6-31+G (d,p)
X	1.354416	α_{xx}	33.351	α_{xx}	-75.5873	β_{xxx}	-190.3815402	γ_{xxxx}	-2820.7463
Y	0.2374846	α_{yy}	29.4754	α_{xy}	-11.5508	β_{yxx}	-282.1947852	γ_{yyyy}	-702.6939
Z	0.1873247	α_{zz}	-2.0061	α_{yy}	-82.337	β_{xyy}	-402.5157965	γ_{zzzz}	-221.3517
μ_{Tot}	1.3878 a.u	α_{Tot}	95.5246 a.u	α_{xz}	2.5251	β_{yyy}	-183.4383415	γ_{xxyy}	-659.9646
				α_{zz}	-82.2968	β_{zxx}	-36.1102523	γ_{xxzz}	-560.1589
				α_{yz}	0.885	β_{zyy}	-128.9800639	γ_{yyzz}	-164.388
				$\Delta\alpha_{\text{Tot}}$	21.6109 a.u	β_{xzz}	-12.681115	γ_{Tot}	-1302.76 a.u
						β_{yzz}	14.6808828		
						β_{zzz}	-42.054238		
						β_{Tot}	782.9381 a.u		
$\mu = 3.5277 \text{ Debye}$		$\alpha = 14.16 \times 10^{-24} \text{ esu}$		$\Delta\alpha = 3.2027 \times 10^{-24} \text{ esu}$		$\beta = 6.7645 \times 10^{-30} \text{ esu}$		$\gamma = -6562.28 \times 10^{-40} \text{ esu}$	

of chemical bond occurs between molecules [58, 59].

The concept of generalized philicity was introduced by Chattaraj et.al [60]. It contains the different global reactivity and local selectivity descriptors and also provides the information regarding electrophilic and nucleophilic power of a given atomic site in a molecule. Recently, the electrophilicity was used to elucidate the toxicity of benzidine and polychlorinated by biphenyls has been assessed.

In addition the different local softness used to describe the reactivity of atoms, can be defined as

$$s_k^\alpha = S f_k^\alpha \quad (19)$$

Where $\alpha = +, -, 0$ represents nucleophilic (S_k^+), electrophilic (S_k^-) and radical attack respectively. The relative nucleophilicity (S_k^-/S_k^+) and relative electrophilicity (S_k^+/S_k^-) indices have been described by using local softness.

The local quantity known as philicity which associated with a site K in a molecule defined as

$$\omega_k^\alpha = \omega f_k^\alpha \quad (20)$$

Where $\alpha = +, -, 0$ represents local philic quantities determining the electrophilic, nucleophilic and radical respectively. The most electrophilic site in a molecule was investigated by using the above equation with providing maximum value of ω_k^- and ω_k^+ .

The local softness, relative electrophilicity, nucleophilicity, dual local softness (Δs_k) and multiphilicity descriptors ($\Delta\omega_k$) with corresponding local reactivity descriptors of the individual atoms of the molecule are presented in Table 6 which are evaluated at B3LYP/6-31+G (d,p) basis set. The atoms C3,C4,C7,F8,F9,H11,H12,O13,H15,H16,H18,H19, C20,H21, H22 and H23 are explicitly for nucleophilic attack and rest of atoms for electrophilic attack which explain clearly the electron rich/deficient nature of the individuals atoms [61].

3.10. Non-linear optical properties

Organic materials have attracted with large optical non-linearities become the fore front of the current research in view of their non

linear optical (NLO) susceptibilities and display a number of significant potential applications in various photonic technologies including all optical switching and in modern communication [62]. Among NLO materials, amino acids contain a proton donor carboxyl acid group and proton acceptor amino group enhance the NLO response [63]. Organic molecules that exhibit extended π -conjugation makes the molecule to be highly polarized. In particular, it shows enhanced NLO characteristics such as frequency doubling or second harmonic generation (SHG) [64, 65].

Second order Non linear optical properties, which are exploited in telecommunications arise in molecules that lack of centre of symmetry [66]. In order to obtain the second order non linearities (hyper-polarizabilities), conjugated organic molecules are substituted with electron-donar and electron-acceptor end groups. Generally β depends on the strength of the donor and acceptor groups with strong electronic coupling through the conjugated π -bridge [67].

The static response properties of a molecule can be expressed by expanding the field-dependent energy E (F) which is expressed by [68].

$$E(F) = E_0 - \sum \mu_i F_i - \frac{1}{2} \sum \alpha_{ij} F_i F_j - \frac{1}{6} \sum \beta_{ijk} F_i F_j F_k - \frac{1}{24} \sum \gamma_{ijkl} F_i F_j F_k F_l - \quad (21)$$

where E is the energy of a molecule under the electric field F, E_0 is the unperturbed energy of a free molecule, F_i is the vector component of the electric field in the i direction and μ_i , α_{ij} , β_{ijk} , γ_{ijkl} are the dipole moment, linear polarizability, first and second order hyper polarizabilities respectively.

The complete equations for calculating the magnitude of dipole moment (μ), polarizability(α), anisotropy of the polarizability ($\Delta\alpha$), first hyperpolarizability (β) and second hyperpolarizabilities (γ) using the x,y,z component are explained as follows [69].

$$\text{Dipole moment } \mu = \left(\mu_x^2 + \mu_y^2 + \mu_z^2 \right)^{\frac{1}{2}} \quad (22)$$

$$\text{Polarizability } \alpha = \frac{\alpha_{xx} + \alpha_{yy} + \alpha_{zz}}{3} \quad (23)$$

$$\Delta\alpha = \frac{1}{\sqrt{2}} \left[(\alpha_{xx} - \alpha_{yy})^2 + (\alpha_{yy} - \alpha_{zz})^2 + (\alpha_{zz} - \alpha_{xx})^2 + 6(\alpha_{xz}^2 + \alpha_{xy}^2 + \alpha_{yz}^2) \right]^{\frac{1}{2}} \quad (24)$$

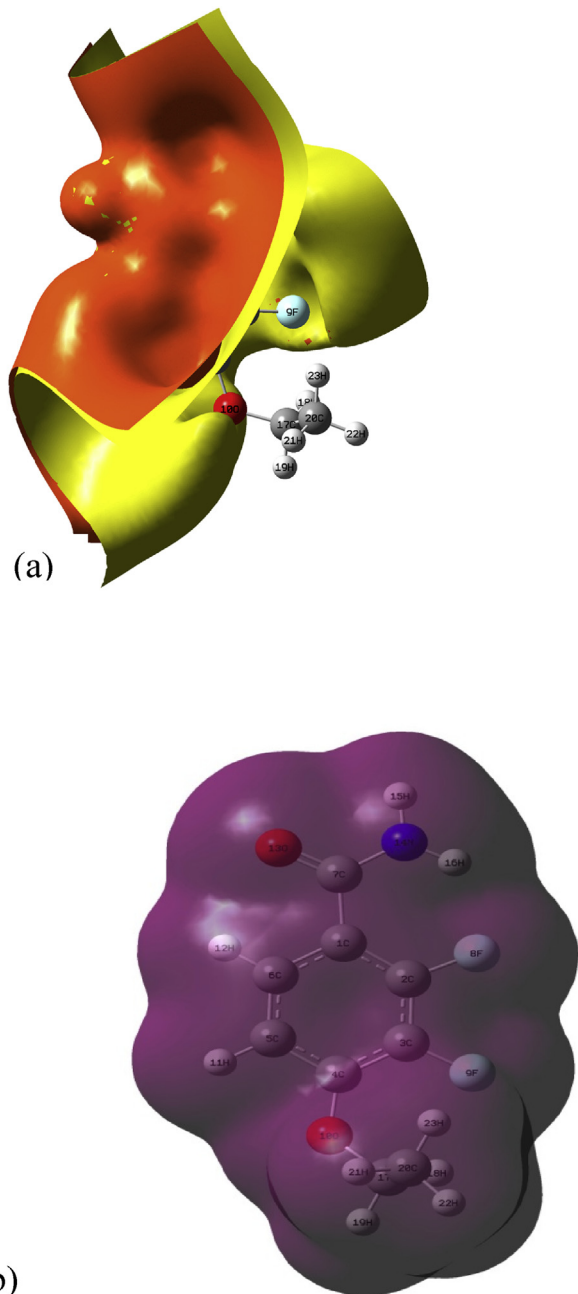


Fig. 8. (a) Electrostatic potential surface and (b) Total electron density of 4-ethoxy -2, 3-difluoro benzamide.

Anisotropic polarizability

$$\text{First hyperpolarizability } \beta = \left(\beta_x^2 + \beta_y^2 + \beta_z^2 \right)^{\frac{1}{2}} \quad (25)$$

Here

$$\beta_x = \beta_{xxx} + \beta_{xyy} + \beta_{xzz}$$

$$\beta_y = \beta_{yyy} + \beta_{xxy} + \beta_{yzz}$$

$$\beta_z = \beta_{zzz} + \beta_{xzx} + \beta_{yyz}$$

In this study, dipole moment, polarizabilities, and the second and third order polarizabilities or hyperpolarizabilities of the title molecule were investigated by using B3LYP at 6-31+G (d,p) basis set. The calculated values of $\mu, \alpha, \Delta\alpha, \beta$ and γ are tabulated in Table 7. The dipole moment resonates molecular charge distribution and it can be describes the charge movement across molecule. The total dipole moment was found to be 3.5277 Debye. In NLO system, the magnitude of the first hyperpolarizability is the most significant factor. The negative value of β indicates that the charge flows in the opposite direction to the dipole moment in the excitation. The domination of hyperpolarizability value in the particular component $\beta_{yyz} = 14.68088$ implies a substantial delocalization of charges in this direction. The average polarizability (α) and first hyperpolarizability (β) are 14.16×10^{-24} esu and 6.7645×10^{-30} esu respectively, which are greater than carbomide. The carbomide is the most archetypical compound for second harmonic generation (SHG) with in the NLO system [70, 71]. Theoretically obtained values of various components ($\mu = 4.2156$ Debye = 3.0045×10^{-24} esu and $\beta = 0.1944 \times 10^{-30}$ esu) of carbomide at B3LYP/6-31+G (d,p) basis set. These results show that the calculated value of first hyperpolarizability of the title molecule is 35 times greater than of carbomide. Hence the title molecule enhances the future potential applications in the development of NLO materials.

3.11. Molecular electrostatic potential (MEP)

It should be noted that any chemical system creates an electrostatic potential around itself. Molecular electrostatic potential (MEP) is very important tool to investigate and correlate between the molecular structure and the physicochemical property relationship of the molecules with including biomolecules and drugs [72]. The electrostatic potential surface was mapped over the electron density which displays the molecular size, shape and charge distribution. It gives information about the molecules interaction with one another and simultaneously ESP has been used extensively for predicting reactive behavior and inter and intra-molecular interaction of chemical systems as well as hydrogen bonding [73]. The significance of MEP provides a visual method to understand the relative polarity of the molecule and simultaneously the different values of the electrostatic potential represented by different colours; blue, red and green represented region of most positive, most negative and zero electrostatic potential, respectively. It means, potential increases in the order blue > green > yellow > orange > red. The negative region (red, orange and yellow) indicates electrophilic reactivity and the positive region to nucleophilic reactivity. Red indicates the strongest repulsion, blue indicates the strongest attraction and green indicates neutral electrostatic potential region. In order to predict reactive sites of electrophilic and nucleophilic attack and for the title molecule, the 3D molecular electrostatic (MEPS) potential and total electron density are illustrated in Fig. 8. In this compound the MEP shows that the negative potential sites on electronegative atoms and the positive potential sites on hydrogen atoms [74].

$$\text{Second order hyperpolarizability } \gamma = \frac{[\gamma_{xxx} + \gamma_{yyy} + \gamma_{zzz} + 2(\gamma_{xxy} + \gamma_{xzz} + \gamma_{yyz})]}{5} \quad (26)$$

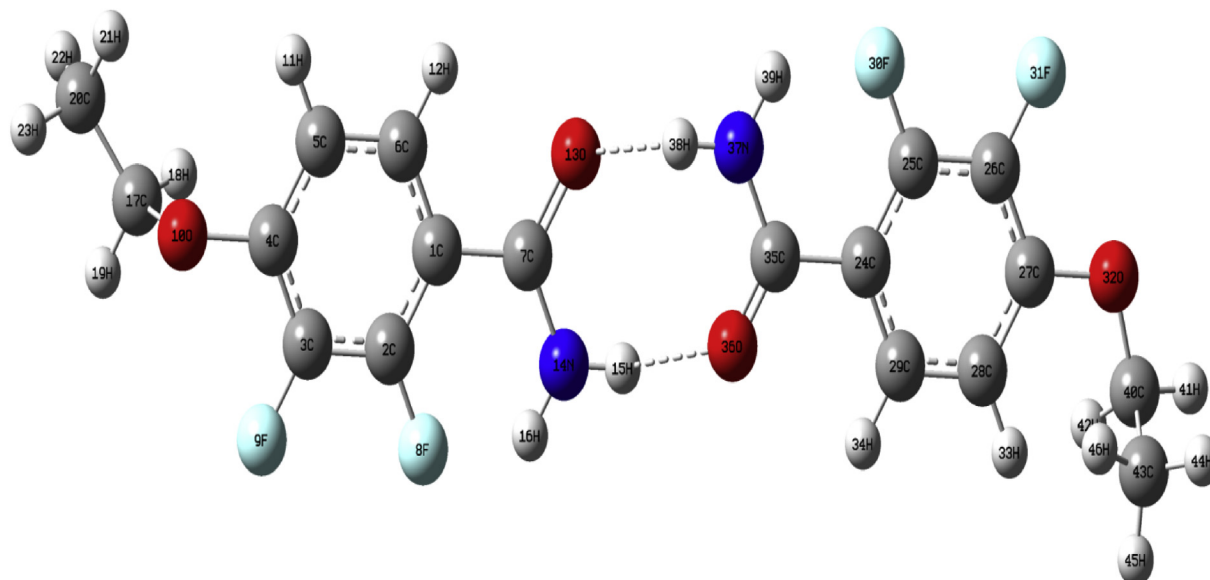


Fig. 9. Dimer structure of 4-ethoxy -2, 3-difluoro benzamide.

Table 8

Intermolecular hydrogen bonding parameter (bond length/ \AA^0) of 4-ethoxy -2, 3-difluoro benzamide based on B3LYP/6-31+G (d, p) method.

O13...H38 - N37	O13 – H38	N37 – H38
	1.736	1.042
N14 – H15 ...O36	O36 – H15	N14 – H15
	1.736	1.042

Table 9

Calculated Mulliken atomic charges of 4 - Ethoxy-2, 3-difluoro benzamide.

Atoms	B3LYP/6-31+G (d,p)
	Mulliken Charges (a.u)
1 C	0.968151
2 C	-0.752525
3 C	0.918079
4 C	-0.259989
5 C	0.100041
6 C	-0.544098
7 C	0.517658
8 F	-0.361913
9 F	-0.364727
10 O	-0.358014
11 H	0.145645
12 H	0.177034
13 O	-0.539148
14 N	-0.595057
15 H	0.332462
16 H	0.317547
17 C	-0.05999
18 H	0.160252
19 H	0.14825
20 C	-0.4245
21 H	0.161473
22 H	0.154336
23 H	0.159033

3.12. Hydrogen bonding

A dimer is an oligomer composed of two structurally similar monomers joined by chemical bonds that can be either covalent or intermolecular. Non covalent dimers namely carboxylic acids, acetic acids and protein dimer can be formed by hydrogen bonding. Hydrogen bonds are

very abundant in nature and they are in inherently present in number of organic and bio-molecules. Hydrogen bond is an important non-covalent interaction in chemistry and biology and which can be divided in to two categories namely intramolecular and intermolecular hydrogen bonds based on donor and acceptors are reside in different manner. In intramolecule hydrogen bonds, the donor and accepter atoms exist in the same molecule and in intermolecular hydrogen bonds, donor and acceptor groups are reside in different molecules [75]. The various strategies are employed to elucidate the in-depth understanding of inter and intra molecular hydrogen bonds. For example, P. Dhanishta et.al studied the existence of intra molecular hydrogen bonds in synthesized benzoyl phenyl oxalamide derivatives using NMR studies and DFT computations [76, 77].

Intermolecular interactions play a pivotal role in biomolecules and drug designs and to interpret the molecular structure and deformability. Particularly, hydrogen bond is evolved in three dimensional conformations of proteins and peptide catalysis [78]. A special type of electrostatic dipole-dipole attraction occurs when hydrogen atom strongly bonded to electronegative atom exists in the vicinity of another electronegative atom such as nitrogen, oxygen or fluorine bearing a lone pair of electrons. Due to this significance, for the present compound the hydrogen bond analysis has been carried out using dimer structure is depicted in Fig. 9 and the corresponding values are shown in Table 8. A remarkable reduction is observed in the intermolecular hydrogen bond lengths ($14\text{N} \cdots 15\text{H} = 37\text{N} \cdots 38\text{H} = 1.04 \text{\AA}^0$ and $13\text{O} \cdots 38\text{H} = 36\text{O} \cdots 15\text{H} = 1.74 \text{\AA}^0$) when compared the sum of van der walls radii ($\text{O} \cdots \text{H} = 2.70 \text{\AA}^0$ and $\text{N} \cdots \text{H} = 2.74 \text{\AA}^0$) which strongly confirms the presence of intermolecular hydrogen bonds [79, 80, 81].

3.13. Mulliken analysis

The Calculation of Mulliken atomic charges have an important role in the application of quantum mechanical calculations to atomic charges which causes dipole moment, molecular polarizability and electronic properties of molecular systems [82]. The positive and negative charge distribution is significant role to increasing or decreasing the bond length between the atoms of the molecule. In order to determine the electron population of each atom calculated by Mulliken charges of 4EDFB using B3LYP/6-31 + G (d,p) basis set and the corresponding values are illustrated in Table 9. The results show that, all hydrogen atoms exhibits positive which are an acceptor and the values varies from 0.1483 to 0.3325. The hydrogen atoms where located at the different functional

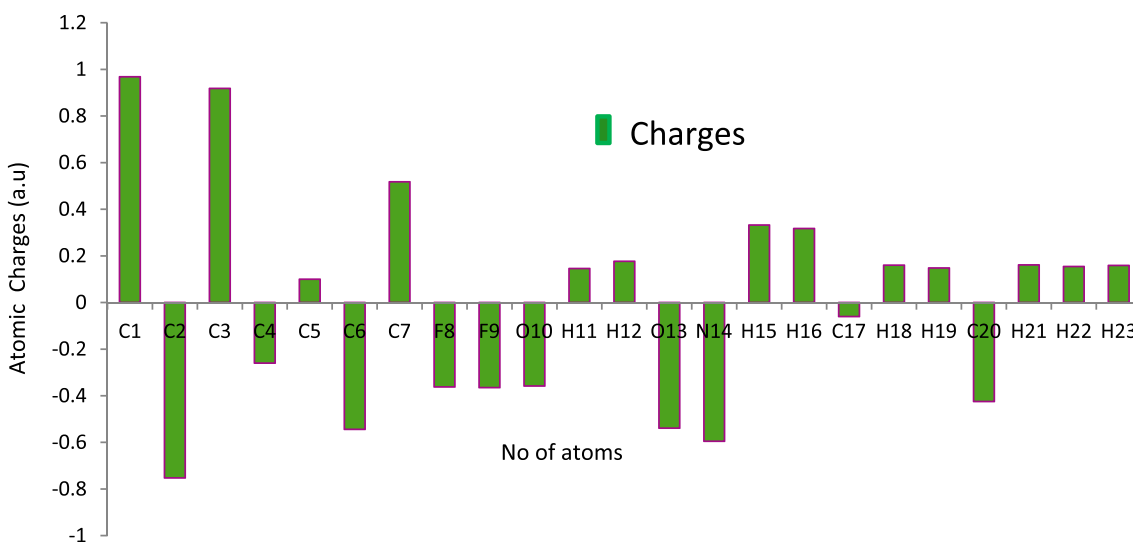


Fig. 10. The graphical representation of Mulliken charges for different atoms of 4-ethoxy-2,3-difluoro benzamide.

group such as methylene ($H_{18} = H_{19}$), methyl ($H_{21} = H_{22} = H_{23}$) and amide groups ($H_{15} = H_{16}$). The highly positive hydrogen atoms H_{15} and H_{16} is due to fact that accepting the electrons from negatively charged nitrogen atom N_{14} . Within the benzene ring, three carbon atoms C_2 , C_4 and C_6 are negative which are donor atoms while rest of three atoms are positive. The highly negative carbon atom C_2 is due to substitution of the highest electronegative atom F_8 which makes the neighboring atoms C_1 and C_3 as positive [83]. The graphical representations of charges are shown in Fig. 10.

4. Conclusion

In the present investigation, the experimental and theoretical vibrational analysis of 4-ethoxy-2,3-difluoro benzamide (4EDB) have been carried out based on scaled quantum mechanical force field approach using Density functional theory. The differences between the scaled and observed values of the fundamentals are very small which are coinciding with experimental results. The vibrational spectral investigation reveals the presence of intra-molecular charge transfer from electron donor to acceptor, which leads to NLO activity of the compound. The NLO activity of the present compound was also confirmed by the predicted large value of first order hyperpolarizability. HOMO-LUMO energy gap enhance the stability of the molecule. The chemical descriptors elucidate the reactivity and site selectivity of the molecule. The different substitution reaction mechanisms of the molecule have been discussed by using Fukui function and local softness. A special type of dipole-dipole interaction was performed using dimer structure. The MEP explicate that the positive and negative potential sites are on around the hydrogen atom and amide group. The net charge distribution of the title molecule was computed by the mulliken population analysis.

Declarations

Author contribution statement

Manivannan Arivazhagan: Conceived and designed the experiments; Contributed reagents, materials, analysis tools or data.

V. Vidhya: Performed the experiments; Wrote the paper.

A. Austine: Analyzed and interpreted the data.

Funding statement

This research did not receive any specific grant from funding agencies in the public, commercial, or not-for-profit sectors.

Competing interest statement

The authors declare no conflict of interest.

Additional information

No additional information is available for this paper.

References

- [1] Prateek Tyagi, Sulekh Chandra, B.S. Saraswat, Ni(II) and Zn(II) complexes of 2-(thiophen-2-ylmethylene)amino benzamide: synthesis, spectroscopic characterization, thermal, DFT and anticancer activities, *J. Spectrochim. Acta A* 134 (2015) 200–209.
- [2] D. Carbonnelle, F. Elstein, C. Rabu, J.Y. Petit, M. Gregoire, F. Lang, A new carbamoyl compound exerts immuno-suppressive activity by inhibiting dendritic cell maturation, *Eur. J. Immunol.* 35 (2005) 546–556.
- [3] Cong-Shan Jiang, Xiao-Meng Wang, San-Qi Zhang, Lie-Su Meng, Wen-Hua Zhu, Jing Xu, She-Min Lu, Discovery of 4-benzoylamino-N-(prop-2-yn-1-yl)benzamides as novel microRNA-21 inhibitors, *J. Bioorg. Med. Chem.* 23 (2015) 6510–6519.
- [4] Minhang Xin, Liandi Zhang, Jun Wen, Shen Han, Zhaoya Liu, Xinge Zhao, Qiu Jin, Mengyu Wang, Lingfei Cheng, Wei Huang, Feng Tang, Synthesis and pharmacological evaluation of trifluoromethyl containing 4-(2-pyrimidinylamino) benzamides as Hedgehog signaling pathway inhibitors, *J. Bioorg. Med. Chem.* 24 (2016) 1079–1088.
- [5] Kaapjoo Park, Byoung Moon Lee, Kwan Hoon Hyun, Dong Hoon Lee, Hyun Ho Choi, Hyunmi Kim, Wonee Chong, Kyeong Bae Kim, Su Youn Nam, Discovery of 3-(4-methanesulfonylphenoxy)-N-[1-(2-methoxyethoxy)methyl]-1H-pyrazol-3-yl-5-(3-methylpyridin-2-yl)-benzamide as a novel glucokinase activator (GKA) for the treatment of type 2 diabetes mellitus, *J. Bioorg. Med. Chem.* 22 (2014) 2280–2293.
- [6] K. Stenlöf, W.T. Cefalu, K.-A. Kim, M. Alba, K. Usiskin, C. Tong, W. Canovatchel, G. Meininger, Efficacy and safety of canagliflozin monotherapy in subjects with type 2 diabetes mellitus inadequately controlled with diet and exercise, *J. Diabetes Obes. Metab.* 15 (2013) 372–382.
- [7] B. Malavasi, M. Locatelli, M. Ripamonti, V. Ascalone, Determination of amisulpride, a new benzamide derivative in human plasma and urine by liquid-liquid extraction or solid-phase extraction in combination with high-performance liquid chromatography and fluorescence detection application to pharmacokinetics, *J. Chromatogr. B* 676 (1996) 107–115.
- [8] M. Bobbot, L. Doare, B. Diquet, Determination of a new benzamide, amisulpride, in human plasma by reversed-phase ion-pair high-performance liquid chromatography, *J. Chromatogr. B* 416 (1987) 414–419.
- [9] Daniela Stark, Markus Piel, Harald Hubner, Peter Gmeiner, Gerhard Grunder, Rosch Frank, In vitro affinities of various halogenated benzamide derivatives as potential radioligands for non-invasive quantification of D2-like dopamine receptors, *J. Bioorg. Med. Chem.* 15 (2007) 6819–6829.
- [10] Yifan Jin, Yanyan Zhu, Mingsheng Tang, Anil Kumar, Balasubramanian Narasimhan, Devinder Kumar, Synthesis, antimicrobial, and QSAR studies of substituted benzamide, *J. Bioorg. Med. Chem.* 15 (2007) 4113–4124.
- [11] Anil Kumar, Balasubramanian Narasimhan, Devinder Kumar, Synthesis, antimicrobial, and QSAR studies of substituted benzamides, *J. Bioorg. Med. Chem.* 15 (2007) 4113–4124.

- [12] V. Krishnakumar, K. Murugeswari, N. Surumbarkuzhal, Molecular structure, intramolecular hydrogen bonding and vibrational spectral investigation of 2-fluoro benzamide - a DFT approach, *J. Spectrochim. Acta A* 114 (2013) 410–420.
- [13] Yaping Tao, Ligang Han, Xiaofeng Li, Yunxia Han, Zhaojun Liu, Molecular structure, spectroscopy (FT-IR, FT-Raman), thermodynamic parameters, molecular electrostatic potential and HOMO-LUMO analysis of 2, 6-dichlorobenzamide, *J. Mol. Struct.* 1108 (2016) 307–314.
- [14] Mehmet Karabacak, Sibel Bilgili, Ahmet Atac, Molecular structure, spectroscopic characterization,HOMO and LUMO analysis of 3,3'-diaminobenzidine with DFT quantum chemical calculations, *J.Spectrochim . Acta A* 150 (2015) 83–93.
- [15] T. Sundius, Scaling of ab initio force fields by MOLVIB, *J. Vib. Spectrosc.* 29 (2002) 89–95.
- [16] M. Karabacak, E. Kose, E.B. Sas, M. Kurt, A.M. Asiri, A. Atac, DFT calculations and experimental FT-IR, FT-Raman,NMR,UV-Vis spectral studies of 3-fluorophenylboronic acid, *J. Spectrochim. Acta A* 136 (2015) 306–320.
- [17] P. Muniappan, R. Meenakshi, G. Rajavel, M. Arivazhagan, Vibrational spectra and theoretical calculations (dimerization, UV-Vis, multinuclear NMR and pes analyses) of 3,4-dimethylbenzamide and 3,4,5-trihydroxybenzamide, *J. Spectrochim. Acta A* 117 (2014) 739–753.
- [18] K. Carthigayan, S. Xavier, S. Periandy, HOMO-LUMO, UV, NLO, NMR and vibrational analysis of 3-methyl-1-phenylpyrazole using FT-IR, FT-Raman FT-NMR spectra and HF-DFT computational methods, *J. Spectrochim. Acta A* 14 (2015) 350–363.
- [19] Satish Chand, Fatmeh A.M. Al- Omary, Ali A. El-Emam, Vikas K. Shukla, Onkar Prasad, Leena Sinha, Study on molecular structure, spectroscopic behavior, NBO, and NLO analysis of 3-methylbezothiazole-2-thione, *J. Spectrochim. Acta A* 146 (2015) 129–141.
- [20] Yaping Tao, Xiaofeng Li, Ligang Han, Weiyi Zhang, Zhaojun Liu, Spectroscopy (FT-IR, FT-Raman), hydrogen bonding, electrostatic potential and HOMO-LUMO analysis of tioxolone based on DFT calculations, *J. Mol. Struct.* 1121 (2016) 188–195.
- [21] Mehmet Karabacak, Leena Sinhab, Onkar Prasad, Zeliha Cinara, Mehmet Cinar, The spectroscopic (FT-Raman, FT-IR, UV and NMR), molecular electrostatic potential, polarizability and hyperpolarizability, NBO and HOMO-LUMO analysis of monomeric and dimeric structures of 4-chloro-3,5-dinitrobenzoic acid, *J.Spectrochim . Acta A* 93 (2012) 33–46.
- [22] M. Arivazhagan, V.P. Subhasini, Quantum chemical studies on structure of 2-amino-5-nitropyrimidine, *J. Spectrochim. Acta A* 91 (2012) 402–410.
- [23] S. Muthu, G. Ramachandran, J. Uma maheswari, Vibrational spectroscopic investigation on the structure of 2-ethylpyridine-4-carbothioamide, *J. Spectrochim. Acta A* 93 (2012) 214–222.
- [24] R. Wysokinski, D. Michalska, D.C. Bienko, S. Ilkiamani, N. Sundaraganesan, K. Ramalingam, Density functional study on the molecular structure, infrared and Raman spectra, and vibrational assignment for 4-thiocarbamoylpyridine, *J. Mol. Struct.* 791 (2006) 70–76.
- [25] A. Yilmaz, O. Bolukbasi, Molecular structure and vibrational spectroscopic studies of prothionamide by density functional theory, *J. Spectrochim. Acta A* 152 (2016) 262–271.
- [26] M. Arivazhagan, R. Kavitha, Molecular structure,vibrational spectroscopic, NBO, HOMO-LUMO and Mulliken analysis of 4-methyl-3-nitro benzyl chloride, *J. Mol. Struct.* 1011 (2012) 111–120.
- [27] B. Latha, S. Gunasekaran, S. Srinivasan, G.R. Ramkumar, Computation and interpretation of vibrational spectra on the structure of Losartan using ab initio and Density Functional methods, *J. Spectrochim. Acta A* 132 (2014) 375–386.
- [28] J. Sharmi Kumar, T.S. Renuga Devi, G.R. Ramkumar, Ab initio and density functional theory calculations of molecular structure and vibrational spectra of 4-(2-Hydroxyethyl) piperazine-1-ethanesulfonic acid, *J. Spectrochim. Acta A* 151 (2016) 509–522.
- [29] G.R. Ramkumar, S. Srinivasan, J.J. Boopathy, S. Gunasekaran, B. Prameena, Vibrational spectroscopic studies on 2'-3'-didehydro-2'-3'-dideoxythymidine using density functional theory method, *J. Mol. Struct.* 1059 (2014) 185–192.
- [30] Vesna D. Vitnik, Zelko J. Vitnik, The spectroscopic (FT-IR, FT-Raman, I3C, 1H NMR and UV) and NBO analyses of 4-bromo-1-(ethoxycarbonyl) piperidine-4-carboxylic acid, *J. Spectrochim. Acta A* 138 (2015) 1–12.
- [31] N. Ramesh Babu, H. Saleem, S. Subashchandrabose, M. Syed Ali Padusha, S. Bharanidharan, Structural and vibrational studies on 1-(5-methyl-[1,3,4] thiadiazol-2-yl)-pyrrolidin-2-ol, *J. Spectrochim. Acta A* 152 (2016) 252–261.
- [32] M. Arivazhagan, J. Senthil kumar, Molecular structure, vibrational spectral assignments, HOMO-LUMO, MESP, Mulliken analysis and thermodynamic properties of 2,6-xenol and 2,5-dimethyl cyclohexanol based on DFT calculation, *J. Spectrochim. Acta A* 137 (2015) 490–502.
- [33] S. Jayavijayan, Molecular structure, spectroscopic (FTIR, FT-Raman, 13C and 1H NMR, UV), polarizability and first-order hyperpolarizability, HOMO–LUMO analysis of 2, 4-difluoroacetophenone, *J. Spectrochim. Acta A* 136 (2015) 553–556.
- [34] S.K. Pathak, R. Srivastava, A.K. Sachan, O. Prasad, L. Sinha, A.M. Asiri, M. Karabacak, Experimental (FT-IR, FT-Raman, UV and NMR) and quantum chemical studies on molecular structure, spectroscopic analysis, NLO, NBO and reactivity descriptors of 3,5-difluorotoluene, *Spectrochim. Acta* 135 (2015) 283–295.
- [35] S. Ramalingam, S. Periandy, B. Elanchezhian, S. Mohan, FT-IR and FT-Raman spectra and vibrational investigation of 4-chloro-2-fluoro toluene using ab initio HF and DFT (B3LYP/B3PW91) calculations, *J. Spectrochim. Acta A* 78 (2011) 429–436.
- [36] M. Arivazhagan, N.K. Kandasamy, G. Thilagavathy, Indian, FT-IR studies on vibrational spectra,HOMO-LUMO,NBO and thermodynamic function analysis of cyanuric fluoride, *J. Pure Appl. Phy.* 50 (2012) 299–307.
- [37] Khaled Bahgat, Safwan Fraihat, Normal coordinate analysis, molecular structure, vibrational, electronic spectra and NMR investigation of 4-Amino-3-phenyl-1H-1,2,4-triazole-5(4H)-thione by ab initio HF and DFT method, *J. Spectrochim. Acta A* 135 (2015) 1145–1155.
- [38] G. Varsanyi, Normal Vibrations of Benzene and its derivatives,Vibrational Spectra of Benzene Derivatives, Academic Press, NewYork, 1969.
- [39] Turgay Polat, Fatih Bulut, Ilknur Arican, Fatma Kandemirli, Gurcan Yildirim, Vibrational assignments, spectroscopic investigation (FT-IR and FT-Raman), NBO, MEP, HOMO–LUMO analysis and intermolecular hydrogen bonding interactions of 7-fluoroisatin, 7-bromoisatin and 1-methylisatin – A comparative study, *J. Mol. Struct.* 1101 (2015) 189–211.
- [40] Erol Tasal, Sidiq Isa, Yadigar Gulseven, Cemil Orgetir, Tijen Onkol, Experimental and density functional theory and ab initio Hartree-Fock study on the vibrational spectra of 5-chloro-6-(4-chlorobenzoyl)-2-benzothiazolinone molecule, *J. Spectrochim. Acta A* 72 (2009) 801–810.
- [41] G. Subhapriya, S. Kalyanaraman, S. Gandhimathi, N. Surumbarkuzhal, V. Krishnakumar, Structural, intramolecular hydrogen bonding and vibrational studies on 3-amino-4-methoxy benzamide using density functional theory, *J. Chem. Sci.* 129 (2017) 259–269.
- [42] Paul Von Rague Schleyer, Haijun Jiao, What is Aromaticity? *J. Pure Appl. Chem.* 68 (1996) 209–218.
- [43] T.M. Krygowski, Crystallographic studies of inter-and intramolecular interactions reflected in aromatic character of. pi-electron systems, *J. Chem. Inf. Comput. Sci.* 33 (1993) 70–78.
- [44] T.M. Krygowski, M. cyranski, Separation of the energetic and geometric contributions to the aromaticity of pi-electron carbocyclics, *J. Tetrahedron* 52 (1996) 1713–1722.
- [45] Ferran Feixas, Eduard Matito, Jordi Poater, Miquel Sola, Aromaticity of distorted benzene rings: exploring the validity of different indicators of aromaticity, *J. Phys. Chem. A* 111 (2007) 4513–4521.
- [46] S.H. Rosline Sebastian, Monirah A. Al-Alshaikh, Ali A. El-Emam, C. Yohannan paniker, Zitko Jan, Marlin Dolezal, C. VanAlsenoy, Spectroscopic, quantum chemical studies, Fukui functions, in vitro antiviral activity and molecular docking of 5-chloro-N-(3- nitrophenyl)pyrazine-2-carboxamide, *J. Mol. Struct.* 1119 (2016) 188–199.
- [47] Luis Humberto Mendoza-Huizar, A theoretical study of chemical reactivity of tartrazine through DFT reactivity descriptors, *J. Mex. Chem. Soc.* 58 (2014) 416–423.
- [48] Francesca Milletti, Loriano Storchi, Gianluca Sforza, Simon cross, Gabriele Cruciani, Tautomer enumeration and stability prediction for virtual screening on large chemical databases, *J. Chem. Inf. Mod.* 49 (2009) 68–75.
- [49] David Pegu, Ngangbam Bedmani Sing, Quantum chemical calculations of molecular structure, electronic, thermodynamic and non-linear optical properties of 2-amino-3-nitro-6-methyl pyridine, *Int. J. Adv. Res.* 1 (2013) 531–538.
- [50] Asit K. Chandra, Minh Tho Nguyen, Use of local softness for the interpretation of reaction mechanisms, *Int. J. Mol. Sci.* 3 (2002) 310–323.
- [51] Weitao Yang, Robert G. Parr, Hardness, softness, and the fukui function in the electronic theory of metals and catalysis, *J. Proc. Natl. Acad. Sci.* 82 (1985) 6723–6726.
- [52] Miquel Torrent-Sucarr, Frank De Proft, Paul Geerlings, Paul W- Ayers, Do the local softness and hardness indicate the softest and hardest regions of a molecule? *Chem. Eur. J.* 14 (2008) 8652–8660.
- [53] Maryam Dehestani, Leila Zeidadabinejad, J. Serb, Preparation and characterization of ZrO₂-supported Fe3O4-MNPs as an effective and reusable super paramagnetic catalyst for the Friedländer synthesis of quinoline derivatives, *J. Chem. Soc.* 80 (2015) 997–1008.
- [54] Nuha Ahmed Wazzan, Fatma Mohamed Mahgoub, DFT calculations for corrosion inhibition of ferrous alloys by pyrazolopyrimidine derivatives, *Open J. Phys. Chem.* 4 (2014) 1–6.
- [55] F. Mendez, J.L. Gazquez, A theoretical study of chemical reactivity of tartrazine through DFT reactivity descriptors, *J. Am. Chem. Soc.* 116 (1994) 9298–9301.
- [56] A. Bendjeddu, T. Abbaz, S. Maache, R. Rehamnia, A.K. Gouasmia, D. Villemin, Quantum chemical descriptors of some P-aminophenyl tetraethylfulvalenes through density functional theory (DFT), *Rasayan. J. Chem.* 9 (2016) 18–26.
- [57] Manju Pandey, S. Muthu, N.M., Nanje Gowda, Experimental and density functional theory study of the vibrational properties of 2-mercaptopbenzimidazole in interaction with gold, *J. Mol. Struct.* 1130 (2017) 511–521.
- [58] Luis Humberto Mendoza-Huizar, Clara Hilda Rios-Reyes, Chemical reactivity of atrazine employing the fukui function, *J. Mex. Chem. Soc.* 55 (2011) 142–147.
- [59] J. Padmanabhan, R. Parthasarathi, M. Elango, V. Subramanian, B.S. Krishnamoorthy, S. Gutierrez-oliva, A. Toro-Labbe, D.R. Roy, P.K. chattaraj, Multiphilic descriptor for chemical reactivity and selectivity, *J. Phys. Chem. A* 111 (2007) 9130–9138.
- [60] Pratim Kumar Chattaraj, Buddhadev Maiti, Utpal Sarkar, Philicity: a unified treatment of chemical reactivity and selectivity, *J. Phys. Chem.* 107 (2003) 4973–4975.
- [61] V. Arjunan, L. Devi, R. Subbalakshmi, T. Rani, S. Mohan, Synthesis, vibrational, NMR, quantum chemical and structure-activity relation studies of 2-hydroxy-4-ethoxyacetophenone, *J. Spectrochim. Acta A* 130 (2014) 164–177.
- [62] D. Arivoli, Fundamentals of non linear optical materials, *Pramana - J. Phys.* 57 (2001) 871–883.

- [63] Nouar Sofiane Labidi, Non-linear optical properties of substituted hexatriene: AM1 and ab initio quantum chemical calculations, *Ope. Acce. Lib. Jour.* 1 (2014) 1–10.
- [64] Kanchana S. Thanthiriyawatte, K.M.Nalin de Silva, Non-linear optical properties of novel fluorenyl derivatives- ab initio quantum chemical calculations, *J. Mol. Struct.* 617 (2002) 169–175.
- [65] Adailton N. Castro, Leonardo R. Almeida, Murilo M. Anjos, R. Guliherme, B. Oliveira Hamilton, Napolitano, Clodoaldo Valverde, Basilio Baseia, High efficiency nonlinear optical chalcone Co-crystal and structure-property relationship, *J. New. Chem. Phys. Lett.* 653 (2016) 122–130.
- [66] S.R. Marder, D.N. Beratan, L.-T. Cheng, Approaches for optimizing the first electronic hyperpolarizability of conjugated organic molecules, *J. Sci. ISSN:* 0036-8075 252 (1991) 103–106.
- [67] Leclercq, E. Zoyer, S.-H. Jang, S. Barlow, V. Geskin, et al., Quantum-chemical investigation of second-order nonlinear optical chromophores: comparison of strong nitrile-based acceptor end groups and role of auxiliary donors and acceptors, *J. Chem. Phys.* 124 (2006) 044510–044517.
- [68] P. Calaminici, K. Jug, A.M. Koster, Density functional calculations of molecular polarizabilities and hyperpolarizabilities, *J. Chem. Phys.* 109 (1998) 7756–7763.
- [69] S. Muthu, T. Rajamani, M. Karabacak, A.M. Asiri, Vibrational and UV spectra, first order hyperpolarizability, NBO and HOMO-LUMO analysis of 4-chloro-N-(2-methyl-2,3-dihydroindol-1-yl)-3-sulfamoyl-benzamide, *J. Spectrochim. Acta A.* 122 (2014) 1–14.
- [70] Reem I. Al-Wabli, K.S. Resmi, Y. Sheena Mary, C. Yohannan Panicker, Mohamed A. Attia, Ali A. El-Emam, C. Van Alsenoy, Vibrational spectroscopic studies, Fukui functions, HOMO-LUMO, NLO, NBO analysis and molecular docking study of (E)-1-(1,3-benzodioxol-5-yl)-4,4-dimethylpent-1-en-3-one, a potential precursor to bioactive agents, *J. Mol. Struct.* 1123 (2016) 375–383.
- [71] Jacqueline M. Cole, Paul G. Waddell, Chick C. Wilson, Judith A.K. Howard, Molecular and supramolecular origins of optical Nonlinearity in *N*-methylurea, *J. Phys. Chem.* 117 (2013) 25669–25676.
- [72] A.M. Mansour, Molecular structure and spectroscopic properties of novel manganese (II) complex with sulfamethazine drug, *J. Mol. Struct.* 1035 (2013) 114–123.
- [73] Dong-Lai Wang, Xiao-Ping Sun, Hong-Tao Shen, Dong-Yan Hou, Yu-Chun Zhai, A comparative study of the electrostatic potential of fullerene-like structures of Au32 and Au42, *J. Chem. Phys. Lett.* 457 (2008) 366–370.
- [74] G. Yildirim, Y. Zalaoglu, C. Kirilmis, M. Koca, C. Terzioglu, A characterization study on 2,6-dimethyl-4-nitropyridine N-oxide by density functional theory calculations, *J. Spectrochim. Acta A* 81 (2011) 104–110.
- [75] Jun rong Zheng, Kyungwon kwak, Xin Chen, John B. Asbury, M.D. Fayer, Formation and dissociation of Intra–Intermolecular hydrogen-bonded Solute–Solvent complexes: chemical exchange two-dimensional infrared vibrational echo spectroscopy, *J. Am. Chem. Soc.* 128 (2006) 2977–2987.
- [76] P. Dhanishta, P. Sai Siva Kumar, Sandeep Kumar Mishra, N. Suryaprakash, Intramolecular hydrogen bond directed stable conformations of benzoyl phenyl oxalamides: unambiguous evidence from extensive NMR studies and DFT-based computations, *J. Rsv. Adv.* 8 (2018) 11230–11240.
- [77] Scancep Kumar Mishra, N. Suryaprakash, Intramolecular hydrogen bonding involving organic fluorine: NMR investigations corroborated by DFT-based theoretical calculations, *J. Mol.* 22 (2017) 423–466.
- [78] Omid Kha kshoor, Aaron J. Lin, Tyler P. Korman, Michad R. Sawaya, Shiou-Chuan Tsai, David Eisenberg, James S. Nowick, X-ray crystallographic structure of an artificial β -sheet dimer, *J. Am. Chem. Soc.* 132 (2010) 11622–11628.
- [79] Xingya Kang, Shigenori Kuga, Limei Wang, Min Wu, Yong Huang, Dissociation of intra/inter-molecular hydrogen bonds of cellulose molecules in the dissolution process: a mini review, *J. Bioresour. Bioprod.* 1 (2016) 58–63.
- [80] G. Subhapriya, S. Kalyanaraman, N. Surumbarukuzhal, S. Vijayalakshmi, V. Krishnakumar, Investigation of intermolecular hydrogen bonding in 2,3,4,5,6 pentafluorobenzoic acid through molecular structure and vibrational analysis – a DFT approach, *J. Mol. Struct.* 1083 (2015) 48–56.
- [81] S.S. Batsanov, Van der Waals radii of elements, *J. Inorg. Mater.* 37 (2001) 871–885.
- [82] R.G. Parr, W. Yang, Quantitative CIDNP evidence for the SH_2 reaction of alkyl radicals with Grignard reagents. Implication to the iron catalyzed Kharasch reaction, *J. Am. Chem. Soc.* 106 (1984) 4048–4049.
- [83] Zeynep Demircioglu, Cigdem Albayrak Kastas, Orhan Buyukgugor, Theoretical analysis (NBO, NPA, Mulliken Population Method) and molecular orbital studies (hardness, chemical potential, electrophilicity and Fukui function analysis) of (E)-2-((4-hydroxy-2-methylphenylimino) methyl)-3-methoxyphenol, *J. Mol. Struct.* 1091 (2015) 183–195.